

3 1176 00120 2846

# NATIONAL ADVISORY COMMITTEE FOR AERONAUTICS

TECHNICAL NOTE

No. 1397

AUG 20 1947

A METHOD FOR NUMERICALLY CALCULATING THE AREA AND  
DISTRIBUTION OF WATER IMPINGEMENT ON THE  
LEADING EDGE OF AN AIRFOIL IN A CLOUD

By Norman R. Bergrun

Ames Aeronautical Laboratory  
Moffett Field, Calif.



Washington

August 1947

N A C A LIBRARY  
LANGLEY MEMORIAL AERONAUTICAL  
LABORATORY  
Langley Field, Va.

TECHNICAL NOTE No. 1397

A METHOD FOR NUMERICALLY CALCULATING THE AREA AND  
DISTRIBUTION OF WATER IMPINGEMENT ON THE  
LEADING EDGE OF AN AIRFOIL IN A CLOUD

By Norman R. Berggren

SUMMARY

A method is presented for determining, by step-by-step integration, the trajectories of water drops around any body in two-dimensional flow for which the streamline velocity components are known or can be computed. The method is general and considers the deviation of the water drops from Stokes' law because of speed and drop size.

The equations are presented in general form and then, to illustrate the procedure, water-drop trajectories are calculated about a 12-percent-thick symmetrical Joukowski profile chosen to simulate an NACA 0012 section.

The method provides a means for the relatively rapid calculation of the trajectory of a single drop without the utilization of a differential analyzer.

In addition, consideration is given to the maximum possible rate of water-drop impingement on a body.

INTRODUCTION

As part of a comprehensive research program directed toward a fundamental understanding of the mechanism of thermal ice-prevention for airplanes, the NACA has undertaken an investigation of the performance of a heated wing or empennage section in specified icing conditions. One of the first essentials of such an investigation is a method for estimating or calculating the area over which water will strike the wing, and the distribution of water impingement over that area.

Previous investigations of this nature have considered the water-drop trajectories about cylinders (references 1 and 2) and those about an airfoil (reference 2). In both of these studies the assumption was made that the water drops were sufficiently small to obey Stokes' law of resistance. A more recent investigation for cylinders (reference 3) shows that, for the velocities of airplanes and the drop sizes frequently present in clouds, Stokes' law does not apply and the force acting on the drop can be determined only from a knowledge of the drag coefficient for spheres.

In reference 3, therefore, the methods of previous investigators are modified to include more accurate values of the drop drag coefficient. Equations are established for the determination of the drop trajectories around cylinders, spheres, and ribbons. These equations are derived in forms suitable for use in a differential analyzer and, by utilizing an analyzer, the trajectories are calculated and plotted.

The designer of a heated wing, desiring to know the rate and area of water impingement on the leading edge in a specified cloud at a given flight speed, might assume that the impingement will be identical to that for a cylinder with a radius equal to the wing leading-edge radius. There is some question, however, as to the accuracy of this assumption for the larger drop sizes and for wing sections with small leading-edge radii. The designer is therefore confronted with the desirability of employing a computation method, preferably without the necessity of a differential analyzer, which will provide some indication of the area and distribution of water impingement.

In this report, the water-drop trajectory equations used in reference 3 have been modified to establish a step-by-step integration method applicable to any two-dimensional flow for which the streamline velocity components are known or can be approximated. If drop trajectories for a large range of airspeeds and drop diameters are required, the computation time is large, and the desirability of access to a differential analyzer becomes evident. The integration method presented herein, however, does permit the calculation of any desired number of trajectories without resort to an analyzer; and it also provides a means for estimating the error which will be incurred by replacing the airfoil by a cylinder with a radius equal to the leading-edge radius of the airfoil. In addition, water-impingement data over the entire airfoil surface can be obtained by the integration method.

## SYMBOLS

## Coefficients

a	radius of a drop, microns ( $3.28 \times 10^{-6}$ ft)
$\bar{a}$	average acceleration of a drop over an interval of time, feet per second per second
$a_n$	acceleration of a drop at the beginning of an interval of time, feet per second per second
B	dimensionless ratio $\left(\frac{C_D R}{24K}\right)$
c	chord of airfoil, feet
C	dimensionless concentration factor
$C_D$	drag coefficient for spheres
E	efficiency of deposition of water drops on a body
K	dimensionless drop-inertia quantity, defined in equation (4)
$K_{cr}$	dimensionless drop-inertia quantity for which no drops impinge upon a body
L	unit length of span of an airfoil
M	intensity of water-drop impingement at a point on the surface of a body, pounds per hour, square foot
$M_T$	rate of water-drop impingement on a body, pounds per hour, foot span
p	nondimensional distance
R	local Reynolds number of a drop relative to the air stream
$R_y$	Reynolds number of a drop moving with free-stream velocity in still air
s	distance along the surface of a body from zero percent chord, feet
S	dimensionless streamline parameter

t	unit of time $\left(\frac{c}{U}\right)$ , seconds
$u_x, u_y, u_z$	velocity components of air, relative to free-stream velocity
U	free-stream velocity of air, feet per second
$v_x, v_y, v_z$	velocity components of a water drop, relative to free-stream velocity
$\bar{v}$	average velocity of a drop over an interval of time, feet per second
w	liquid water content of the air, grams per cubic meter ( $62.4 \times 10^{-6}$ , lb/cu ft)
x, y, z	rectangular coordinates, feet
$y_{max}$	maximum ordinate of airfoil
$\alpha$	condition for which no drops will strike a body
$\beta$	proportionality factor
$\Delta$	increment
$\epsilon$	thickness parameter for transforming a circle into a Joukowski airfoil
$\theta, r$	coordinates of a circle of which the origin is at the center
$\lambda_s$	range of a drop in still air, feet
$\mu$	absolute viscosity of air, pounds mass per second, foot
$\rho$	density of a water drop, pounds per cubic foot
$\rho_1$	density of air, pounds per cubic foot
$\psi$	stream function
Subscripts	
o	denotes starting conditions where time is counted as zero

- 1 denotes one interval of time  
 cr denotes a critical condition  
 n denotes nth interval of time  
 n+1 denotes interval of time of (n+1)

## ANALYSIS

To obtain area and concentration of water-drop impingement at the leading edge of an airfoil, the path of the drops as affected by the air stream must be traced. In order to compute these paths, or trajectories, it is necessary to define the motion of a drop through the air. The equations which depict this motion, and which have been modified to include the effect of a drop departing from Stokes' law of resistance have been shown by Langmuir and Blodgett in reference 3 to take the following form:

$$Kv_x \frac{dv_x}{dx} = \frac{C_D R}{24} (v_x - u_x) \quad (1)$$

$$Kv_y \frac{dv_y}{dy} = - \frac{C_D R}{24} (v_y - u_y) \quad (2)$$

$$\frac{dx}{dt} = - v_x$$

$$\frac{dy}{dt} = v_y$$

$$\left(\frac{R}{RU}\right)^2 = (v_x - u_x)^2 + (v_y - u_y)^2 \quad (3)$$

The dimensionless quantity  $K$ , used by Glauert (reference 2), is evaluated by the equation

$$K = \frac{2}{9} \left(\frac{\rho}{\rho_1}\right) \left(\frac{a}{c}\right)^2 \left(\frac{\rho_1 U_c}{\mu}\right) \quad (4)$$

where in a system of consistent units,  $\rho$  is density of the drop,  $\rho_1$  is density of air,  $a$  is radius of the drop,  $U$  is free-stream velocity,  $\mu$  is absolute viscosity of air, and  $c$  is the chord of the airfoil.

It can be seen from equations (1) and (2) that

$$\frac{dv_x}{dt} = - \frac{C_D R}{24K} (v_x - u_x)$$

$$\frac{dv_y}{dt} = - \frac{C_D R}{24K} (v_y - u_y)$$

Since the average velocity of a drop over a small interval of time may be expressed by

$$\bar{v} = \frac{v_{n+1} + v_n}{2}$$

and the average acceleration by

$$\bar{a} = \frac{a_{n+1} + a_n}{2}$$

the velocity and position of a drop at the end of any interval of time may be expressed by the following equations:

$$v_{x(n+1)} = v_{x_n} - \frac{C_D R}{24K} (v_{x_n} - u_{x_n}) \Delta t \quad (5)$$

$$v_{y(n+1)} = v_{y_n} - \frac{C_D R}{24K} (v_{y_n} - u_{y_n}) \Delta t \quad (6)$$

$$x_{(n+1)} = v_{x_n} \Delta t - \frac{1}{2} \left[ \frac{C_D R}{24K} (v_{x_n} - u_{x_n}) \right] \Delta t^2 + x_n \quad (7)$$

$$y_{(n+1)} = v_{y_n} \Delta t - \frac{1}{2} \left[ \frac{C_D R}{24K} (v_{y_n} - u_{y_n}) \right] \Delta t^2 + y_n \quad (8)$$

where the subscript  $n$  denotes a point at the beginning of some interval of time, and the subscript  $n+1$  denotes a point at the end of that interval of time. The main assumption made in these equations is that the acceleration of the drop is constant over the interval of time selected.

Equations (3), (5), (6), (7), and (8) may be used to calculate the trajectory of a drop by a step-by-step process, provided that a sufficient range in values of air-velocity components  $u_x$ ,  $u_y$ , and the drag coefficient function  $C_D R/24$  are available. When Stokes' law of resistance holds, the value of  $C_D R/24$  is unity. The quantities  $u_x$ ,  $u_y$ , and  $C_D R/24$ , are best used in large-scale plots to insure a fair degree of accuracy in the computations. In addition to the large-scale plots required, certain assumptions must be made in regard to the conditions of a drop at the start of its trajectory. This information is needed in order to continue with the step-by-step computations. It appears that the simplest manner in which to start the computations is by assuming the velocity of the drop to be the same as that of the air at a fairly large distance forward of the airfoil, and then estimating the velocity differentials  $v_x - u_x$  and  $v_y - u_y$  between the air and the drop at a new point. An estimation of the magnitude of these differences may be made by the following equations which are derived in appendix A:

$$v_{x_1} = \frac{(u_{x_0} + B\Delta x) \pm \sqrt{(u_{x_0} + B\Delta x)^2 - 4Bu_{x_1}\Delta x}}{2} \quad (9)$$

$$v_{y_1} = \frac{-(B\Delta y - u_{y_0}) \pm \sqrt{(B\Delta y - u_{y_0})^2 + 4Bu_{y_1}\Delta y}}{2} \quad (10)$$



If  $y_0$  is the ordinate of a trajectory for a given drop size at infinity, the quantity of water per unit time and area which progresses toward a body is

$$UwLy_0$$

Since this same amount of water distributes itself over the leading edge of the body, then,

$$UwLy_0 = MLs$$

and for a small increment

$$M = Uw \frac{dy_0}{ds} \quad (11)$$

Since  $dy_0/ds$  is proportional to the concentration of water impingement at various points on a body in a water cloud, it can be appropriately called a concentration factor. Thus,

$$M = UwC \quad (12)$$

The total water collected by a body is the summation of all the degrees of concentration of water-drop impingement over the leading edge of a body for a unit length of span such that

$$M_T = \int_0^S Ms = Uw_{\max} E \quad (13)$$

In equation (13),  $E$  is efficiency of water disposition over the leading edge, and is defined in terms of the maximum ordinate of the body, so that

$$E = \frac{y_{0\text{limit}}}{y_{\max}} \quad (14)$$

where  $y_{0\text{limit}}$  is the ordinate of a starting trajectory which just impinges upon the airfoil, and  $y_{\max}$  is the maximum ordinate of the body.

When drops are quite small, they have insufficient momentum to carry them to the body, hence, there is a critical size of drop which

possesses just sufficient energy to impinge upon the body. This critical condition is given by

$$\alpha = K_{cr} \frac{du_x}{dx} = \frac{1}{4} \quad 1(15)$$

To determine the critical drop size (i.e., the critical K value), it is only necessary to evaluate the quantity  $du_x/dx$  at the stagnation point of the airfoil. Because the quantity  $du_x/dx$  is a property of the streamlines around a body at the stagnation point, it has different values dependent upon the body chosen.

#### COMPUTATION PROCEDURE

The example given herein to explain the computation procedure is for a symmetrical Joukowski airfoil, 12 percent thick, at  $0^\circ$  angle of attack. This airfoil was chosen because the streamline functions could be calculated with relative ease, and because its profile closely simulated that of an NACA 0012 airfoil. Trajectory data for an NACA 0012 section were needed in connection with thermal ice-prevention heat-transfer computations.

Streamlines were obtained about the Joukowski airfoil for a region estimated to cover the paths of drops of particular interest. The equations used to define the contour of the streamlines and the values of velocity components along streamlines were derived from Glauert (reference 4). These equations are given in appendix C.

Streamlines calculated for the Joukowski airfoil are shown in figure 1. In addition, the contour of the NACA 0012 airfoil is presented to show its comparison with the Joukowski profile over the region where it was expected that trajectories would hit for drop sizes typically found in nature.

Air-velocity-component data were used in the forms shown in figures 2(a), 2(b), 2(c), 2(d), and 3. Figure 2(a) gives the x-component of air velocity in terms of the x-coordinate in the vicinity of the airfoil, while figure 2(b) presents the same parameters several chord lengths forward of the airfoil. Figure 2(c) depicts the y-component of velocity in terms of the y-coordinate in a region near the airfoil. However, because of their small magnitudes, y-components

---

<sup>1</sup>Derived in appendix B.

of velocity well forward of the airfoil had to be treated somewhat differently than x-velocity components in order to obtain values sufficiently accurate. It was found that the y-velocity components showed a good degree of change with respect to a change in ratios of the coordinates at any point. It was therefore found desirable to plot the y-velocity components in the manner shown in figures 2(d) and 3. Both x- and y-velocity components were plotted so that their values could be obtained to four significant figures.

Because a water-drop trajectory can cross streamlines, and because air-velocity components are conveniently plotted in terms of streamlines, it is imperative to be able to interpolate between the streamlines to ascertain on what streamline a drop is located at a given time. Interpolation between streamlines can be accomplished by plotting points on streamlines in terms of ratios of the point coordinates. Figure 4 shows the relationship obtained when this was done. The simplicity of this method of interpolation lay in the fact that the streamlines displayed a logarithmic separation, which permits the interpolation to be carried on by laying a logarithmic scale properly across the streamlines. It should be observed that, as a trajectory approaches the ordinate axis (taken in the computations to originate at the stagnation point), the ratio of the coordinates asymptotically approaches infinity. Therefore, in performing the step-by-step computations, it is advisable to abandon this interpolation procedure when values of the coordinate ratio are of the order of 1200 percent. For small values of  $x/c$  forward of the airfoil, the value of the stream function can be obtained for the drop with the aid of the information given in figure 1.

Values of the drop drag-coefficient function  $C_{DR}/24$  and  $R$  were obtained from reference 3, and plotted to a suitable scale for use in the computations. These values are given in table I. As the step-by-step process progresses, new values of  $R$  and  $C_{DR}/24$  are selected from the plots.

From equations (3), (5), (6), (7), and (8) it is apparent that trajectories can be calculated for both ranges of  $K$  and  $R_U$  values, where  $R_U$  is defined by

$$R_U = \frac{2aU_0^3}{\mu}$$

However, because of limited time available for performing the calculations, a set of trajectories (corresponding to several  $K$

values) was computed for only an  $R_{ij}$  value of 95.65. The value of  $R_{ij}$  was chosen because it corresponded to certain airspeed, altitude, and drop-size conditions of particular interest.

Starting coordinates of trajectories were arbitrarily chosen for selected  $K$  values. As an example, by means of equations (9) and (10), for a  $K$  value of 0.0581 and starting coordinates  $x_0=210$  percent chord,  $y_0=0.750$  percent chord, it was determined that

$$-(v_{x_1} - u_{x_1}) = 0.0001$$

$$v_{y_1} - u_{y_1} = 0.1 \times 10^{-5}$$

$$-v_{x_1} = 0.9979$$

$$v_{y_1} = 1.5 \times 10^{-5}$$

$$\frac{C_{pR}}{24} = 1.001$$

$$R_{ij} = 95.65$$

A sample calculation for obtaining these values is shown in appendix D. With these values as starting values, a continuation of the computations is shown in table II for the trajectory. This table expresses equations (3), (5), (6), (7), and (8) in a convenient computational form and is used in conjunction with figures 1, 2(a), 2(b), 2(c), 2(d), 3, and 4.

## RESULTS

From calculations to determine the trajectories of water drops, the area and distribution of water impingement over the leading edge of an airfoil can be obtained. In addition, the total amount of water per unit length of span can be calculated.

If trajectories for one  $Ry$  value are plotted in the manner shown in figure 5, the distance along the surface to the stagnation point included by a trajectory may be measured. Then by taking included distances from a large-scale plot similar to figure 5, a figure like that shown in figure 6 is obtained. The limiting trajectories beyond which no drops will impinge upon the airfoil surface may be obtained by connecting the end points for the several computed trajectories. This is shown by a broken line in figure 6. It is interesting to note in figure 6, that for the case of  $K=\infty$ , the problem reduces to one of plotting the airfoil ordinates against the included surface distances.

By obtaining the slopes of the curves in figure 6, according to equation (11), the concentration factor  $C$  may be obtained at different points over the leading edge of the airfoil. This operation was performed graphically, and the results are shown in figure 7.

The ratio of the limit starting ordinates of trajectories  $Y_{\text{limit}}$  to the maximum ordinate of the airfoil defines the efficiency of drop impingement (equation (14)). Therefore, when such ratios are obtained by means of figure 6, and plotted with respect to their corresponding  $K$  values, an indication of the efficiency of water deposition on an airfoil can be obtained. The value of  $K$  corresponding to zero impingement was estimated to be approximately 0.0009 by means of equation (15). The value of  $du_x/dx$  needed to estimate this value of  $K$  was determined graphically by using a large plot of figure 2(a). A presentation of the efficiency of water-drop impingement on the Joukowski airfoil, for a value of  $Ry=95.65$ , is shown in figure 8.

As a matter of interest, the paths of several drops of different inertia but the same starting points were obtained in relation to the velocity field about the airfoil. These relations are shown in figures 9(a) and 9(b), and were obtained by noting from the computations (as performed by the procedure suggested in table II) the corresponding air-velocity components at different times during a drop trajectory.

#### DISCUSSION

The procedure demonstrated herein for calculating water-drop trajectories about a body in two-dimensional flow is convenient to use when aid from a differential analyzer is not available. In the use of the method, however, certain errors are involved. One of the errors is involved in the ability to predict, with reasonable accuracy,

the starting values of the velocity differentials  $v_{x_1}-u_{x_1}$  and  $v_{y_1}-u_{y_1}$  for small drop sizes ( $K$  values less than approximately 0.02). It appears that, in order to calculate trajectories for these small drops, either the air-velocity components must be obtained to great accuracy or else a better method of approximating the starting values of the differentials must be derived. Another error lies in the accumulation, during successive integration steps, of errors involved by the assumption of an average constant acceleration over the time interval selected. Near the airfoil, errors accumulate more rapidly than they do well forward of the airfoil because of the increased rate at which values of the air-velocity components change. (See figs 9(a) and 9(b).) Large changes in air-velocity components mean large changes in selected values of  $C_D R/24$  which multiply the velocity differentials  $v_x-u_x$  and  $v_y-u_y$ . Therefore, it is desirable to reduce the magnitude of the arbitrary time interval when a trajectory approaches the leading edge. To determine a suitable time interval to apply in the computation of a trajectory as it approaches a body, a criterion is to permit the drop to travel, in the time interval selected, a distance in which the air-velocity x-component values do not change by more than approximately 10 percent.

To greatly reduce the amount of work involved in computing a set of trajectories, starting ordinates of trajectories can be taken very close to the body, and time intervals can be chosen as large as is commensurate with the criterion for their selection. When this was done for the computation given in table II (the starting ordinate being taken at half a chord length forward of the airfoil), area of water-drop impingement was reduced 15 percent. To start the calculations so near the airfoil, it was assumed the drop followed the streamline up to the starting point. Because of this assumption the starting ordinate was large by approximately 10 percent, compared to 2 percent for the computations given in table II.

With the set of trajectories calculated by the step-by-step process and presented in figure 6, a comparison can be made between the impingement of water drops on the Joukowski airfoil and its equivalent cylinder for a small range in drop sizes. Such a comparison is made in figure 10, where the airfoil was used as the basis for comparison. For area of impingement, the equivalent cylinder can be used without much error to a drop-size diameter of approximately 20 microns. However, for rate of impingement, appreciable difference is not encountered until drop diameters are above 15 microns. It is of interest to note that meteorological data obtained in flight

(reference 5) indicate a mean-effective drop-size diameter<sup>2</sup> for cumulus clouds of 15 to 25 microns. Furthermore, mean-effective drop diameters as high as 50 microns have been measured in clouds of the altostratus category. Since, in accordance with the definition of mean-effective drop diameter, half the water contained in a cloud sample is composed of drops larger than the mean-effective diameter, it is apparent that the use of an equivalent cylinder may be subject to considerable error when applied to typical icing conditions in which large drop-size diameters have been observed.

The method for computing trajectories of water drops in two-dimensional flow can be extended to the case of three-dimensional flow about a body of any shape. To extend the method, the trajectory of a drop must be expressed for the third plane. The additional trajectory equations needed are:

$$Kv_z \frac{dv_z}{dz} = - \frac{C_D R}{24} (v_z - u_z) \quad (16)$$

$$\frac{dz}{dt} = v_z$$

In addition, equation (3) which connects the variable drag coefficient  $C_D$  with the local Reynolds number of the drop at a given time becomes:

$$\left( \frac{R}{RU} \right)^2 = (v_x - u_x)^2 + (v_y - u_y)^2 + (v_z - u_z)^2 \quad (17)$$

Thus when equation (16) is placed in forms similar to equations (5), (6), (7), and (8) in the analysis, and equation (17) is solved in a

---

<sup>2</sup> Mean-effective drop diameter as used in the present report is the size of drop in a cloud sample for which the amount of liquid water existing in water drops larger than that drop is equal to the amount of liquid water existing in drops smaller than the drop.

---

manner similar to that indicated in table II, a three-dimensional case may be handled by step-by-step integration when air-velocity components and starting conditions are known. Application of trajectory computations for three-dimensional flow can be made to the case of windshield ice prevention, where it is desirable to know the rate at which water impinges upon a windshield in determining heat requirements to keep a windshield clear of ice. Equations (16) and (17) are basic ones which can be adapted also for use with a differential analyzer.

The concentration factor  $C$  in equation (12) for the three-dimensional case is now evaluated by

$$C = \frac{dA_O}{dA_S} \quad (18)$$

In equation (18),  $A_O$  is an area which is outlined by several starting trajectories; and  $A_S$  is the area, on the surface of the body, which is outlined when these trajectories intercept the body.

The rate of water impingement  $M_T$  in equation (12) is evaluated for the three-dimensional case by

$$M_T = UWEA_{\text{frontal}} \quad (19)$$

In equation (19),  $E$ , the efficiency of water-drop deposition on the body, is now expressed by

$$E = \frac{A_{\text{olimit}}}{A_{\text{frontal}}}$$

where  $A_{\text{olimit}}$  is the area included by starting trajectories which just impinge upon the body, and  $A_{\text{frontal}}$  is the frontal area of the body.



As has already been mentioned, the limit distribution of water-drop impingement on the leading edge of a body can be obtained from the body ordinates. It is interesting to observe that, for very high speeds, the limit condition  $K=\infty$  is approached. Hence, it is believed that a comparison of the water-drop impingement over several different airfoils for the limit condition is of interest. Such a comparison is made in figure 11. For these limit conditions, any body having a leading-edge radius will have a value of the concentration factor at the leading edge of unity; whereas, any body without a leading-edge radius will have a much lower value of the concentration factor depending upon the slope of the contour near the stagnation point. According to equation (13), the area under the curves in figure 11 is proportional to rate of icing per unit span, and in accord with theory, for airfoils with the same value of maximum thickness, regardless of location, the areas under the curves in figure 11 are equal. The difference between each of the three airfoils lies in the manner in which water drops distribute themselves over the airfoil. The reason for this difference is because a limiting water-impingement distribution corresponds to the case where drops are either so large or are traveling so fast that they are undeflected by forces in the air stream. Therefore, the effect of shifting the location of maximum thickness is to change the degree and position of water-drop impingement. Thus the limit water-drop-impingement distribution for a given body can be made to have any desired profile by the proper combination of contour and location of maximum thickness.

#### CONCLUSIONS

From the method outlined in this report to obtain trajectories of water drops forward of a body, the following conclusions can be drawn:

1. By a step-by-step process which considers deviations from Stokes' law of resistance, the area and distribution of water-drop impingement on a body of any shape and angle of attack can be calculated when the air-velocity components are known.
2. The rate and area of water-drop impingement on an NACA 0012 airfoil having an 8-foot chord is approximated with reasonable accuracy by the impingement on a cylinder of radius equal to the leading-edge radius of the airfoil for only drop diameters below 20 microns at speeds of about 200 miles per hour and at an altitude of 7000 feet.

3. The critical drop-size diameter corresponding to zero impingement can be determined for a two-dimensional body if the velocity components are known at the stagnation point.

4. The area and distribution of water-drop impingement on an airfoil in motion through a cloud of known drop-size distribution can be obtained by calculating the area and distribution of impingement for each drop-size range present.

5. Thin airfoils of different sections (such as wedge-shape, NACA 0006, and circular-arc airfoils), having the same exposed frontal areas, will have approximately the same rates of water-drop impingement at high speeds, but the distribution of water-drop impingement will be different for each section, and will depend upon the rate of change of the slope of the airfoil surface and the location of maximum thickness.

Ames Aeronautical Laboratory,  
National Advisory Committee for Aeronautics,  
Moffett Field, Calif., July 1947.

## APPENDIX A

## Derivation of Starting-Point Equations

At a position  $x_0, y_0$  well forward of the airfoil, it is assumed that a drop is moving with a free-stream velocity  $u_x$ . Then

$$u_{x_0} = v_{x_0} \quad (A1)$$

$$u_{y_0} = v_{y_0}$$

The position of the drop after an interval of time  $\Delta t$  is

$$x_1 = x_0 + \Delta x$$

$$y_1 = y_0 + \Delta y$$

where  $\Delta y$  may be expressed in terms of  $\Delta x$  by

$$\Delta y = \frac{u_{y_0}}{u_{x_0}} (\Delta x) \quad (A2)$$

The velocity of a drop, starting initially from a point  $x_0, y_0$ , after an interval of time  $\Delta t$  is

$$v_{x_1} = v_{x_0} + \Delta v_x \quad (A3)$$

$$v_{y_1} = v_{y_0} + \Delta v_y$$

From basic trajectory equations

$$v_x dv_x = B (v_x - u_x) dx \quad (A4)$$

where

$$B = \frac{C_{DR}}{24K}$$

By substituting equations (A1) and (A3) into equation (A4)

$$v_{x1} (v_{x1} - u_{x0}) = B (v_{x1} - u_{x1}) \Delta x$$

and by solving for  $v_{x1}$ ,

$$v_{x1} = \frac{(u_{x0} + B\Delta x) \pm \sqrt{(u_{x0} + B\Delta x)^2 - 4Bu_{x1} \Delta x}}{2} \quad (A5)$$

In a manner similar to that by which equation (A5) was derived, the initial value of the y-component of the drop velocity  $v_{y1}$  may be obtained. The value of  $v_{y1}$  becomes

$$v_{y1} = \frac{-(B\Delta y - u_{y0}) \pm \sqrt{(B\Delta y - u_{y0})^2 + 4Bu_{y1} \Delta y}}{2} \quad (A6)$$

## APPENDIX B

Derivation of Equations for the Condition Where  
No Drops Impinge Upon a Body

In deriving the relationships which describe the limiting value of  $K$  below which no drops will impinge upon a body, it is necessary to consider the basic trajectory equations and the flow field at the stagnation point of the body.

Near the stagnation point of a body, the velocity of both air and of drops which nearly follow the streamlines is so small that  $C_D R/24$  may be taken as unity. In addition, the air-velocity components are nearly linear in relation to their distance from the stagnation point. Glauert shows in reference 2 that  $K$  is proportional to the range of a drop in still air; and in reference 3, Langmuir denotes this range by  $\lambda_S$ , where

$$K = \frac{\lambda_S}{c}$$

Since  $K$  is a function of the air-velocity components and because, near the stagnation point of the body  $x$ -components of air velocity, according to reference 3, may be simplified to

$$u_x \approx \alpha p \tag{B1}$$

and the range of a drop may be written in terms of a distance  $p$  forward of the stagnation point of a body. This distance is defined by

$$p = \frac{cx}{\lambda_S} \tag{B2}$$

Equation (1) may be written

$$Kv_x \frac{dv_x}{dx} = v_x - \alpha p \tag{B3}$$

To solve equation (B3),  $v_x$  may be replaced in manner similar to  $u_x$  by

$$v_x = \beta p \quad (B4)$$

where by differentiating

$$dv_x = \beta dp + p d\beta$$

Then

$$\frac{dv_x}{dp} = \beta + p \frac{d\beta}{dp} \quad (B5)$$

By differentiating equation (B2) with respect to  $x$ ,

$$K dp = dx \quad (B6)$$

and by substituting equations (B4) and (B6) into equation (B3),

$$\frac{dv_x}{dp} = 1 - \frac{\alpha}{\beta} \quad (B7)$$

By setting equations (B5) and (B7) equal to each other and rearranging terms,

$$\frac{dp}{p} = - \frac{\beta d\beta}{\alpha - \beta + \beta^2} \quad (B8)$$

For the integration of equation (B8), Pierce's tables (reference 6) gives

$$\int \frac{\beta d\beta}{\alpha - \beta + \beta^2} = \frac{\ln X}{2h} - \frac{g}{2h} \int \frac{d\beta}{X} \quad (B9)$$

↑  
Misprint!

where

$$X = \alpha + g\beta + h\beta^2$$

and

$$\int \frac{d\beta}{X} = \frac{2}{\sqrt{e}} \tan^{-1} \left( \frac{2h\beta + g}{\sqrt{e}} \right)$$

In equation (B9)

$$e = 4ah - g^2$$

Since  $g=1$  and  $h=1$ , equation (B8) becomes

$$- \ln p = \frac{1}{2} \ln(\alpha - \beta + \beta^2) - \frac{1}{\sqrt{4\alpha - 1}} \tan^{-1} \left( \frac{2\beta - 1}{\sqrt{4\alpha - 1}} \right) \quad (B10)$$

In equation (B10), it is apparent that  $\alpha = \frac{1}{4}$  is a critical value in evaluating the function of  $p$ .

A substitution of equation (B1) into equation (B2) gives

$$Ku_x = \alpha x$$

and by differentiating with respect to  $x$ ,

$$K_{cr} \frac{du_x}{dx} = \alpha$$

Since equation (B10) is dependent solely upon the trajectory equations, the value of  $\alpha$  may always be taken as  $1/4$  in evaluating the critical  $K$  value below which no drops will impinge on a body.

However, the quantity  $du_x/dx$  is dependent upon the shape of a body, the attitude of the body in the air stream, and the type of flow around the body. It, therefore, must be evaluated at the stagnation point for the flow around the body under consideration.

## APPENDIX C

Equations for Obtaining Streamlines and Velocity  
Components about a Symmetrical Joukowski  
Airfoil, 12 Percent Thick

The contour of a streamline is given by

$$x = (r \cos \theta + \epsilon) \left( 1 + \frac{1}{r^2 + \epsilon^2 + 2r\epsilon \cos \theta} \right)$$

$$y = (r \sin \theta) \left( 1 - \frac{1}{r^2 + \epsilon^2 + 2r\epsilon \cos \theta} \right)$$

in which

$$r = \frac{s}{2 \sin \theta} + \sqrt{\left( \frac{s}{2 \sin \theta} \right)^2 + (1 + \epsilon)^2} \quad (C1)$$

In equation (C1)

$$s = - \frac{\psi}{U}$$

where  $\psi$ , a stream function, can have any desired value. In addition, for a symmetrical Joukowski airfoil, 12 percent thick, the value of  $\epsilon$  is 0.1021.



The components of air velocity in terms of free-stream velocity are given by

$$u_x = u_1 u_2 - v_1 v_2$$

$$u_y = u_1 v_2 + u_2 v_1$$

where

$$u_1 = 1 - \frac{(1+\epsilon)^2}{r^2} \cos 2\theta$$

$$v_1 = - \frac{(1+\epsilon)^2}{r^2} \sin 2\theta$$

$$u_2 = \left[ \frac{D(D-1)+F^2}{(D-1)^2+F^2} \right] \quad (C2)$$

$$v_2 = \left[ \frac{F}{(D-1)^2+F^2} \right] \quad (C3)$$

In equations (C2) and (C3),

$$D = r^2 \cos 2\theta + 2 r \epsilon \cos \theta + \epsilon^2$$

$$F = 2r \sin \theta (r \cos \theta + \epsilon)$$

## APPENDIX D

Computation of Starting Values for the  
Step-by-Step Computations.

According to equation (A5), the x-velocity component of a drop is

$$v_{x_1} = \frac{(u_{x_0} + B\Delta x) \pm \sqrt{(u_{x_0} + B\Delta x)^2 - 4Bu_{x_1}\Delta x}}{2}$$

In order to obtain starting values with this equation, this equation must be solved by a trial-and-error method. A procedure for a trial-and-error solution is demonstrated for the starting values used in table II.

For the conditions of table II,

$$x_0 = 2.1; y_0 = 0.0075$$

$$K = 0.0581; R_U = 95.65$$

Several chord lengths forward of the airfoil, as a first approximation, the quantity  $v_{y_1} - u_{y_1}$  may be considered zero. Thus

$$R \approx \pm R_U (v_{x_1} - u_{x_1})$$

Assuming a value of  $-(v_{x_1} - u_{x_1}) = 0.0001$ , the value of  $R$  is

$$R \approx 0.00956$$

for which the value of  $C_D R/24$  is

$$\frac{C_D R}{24} \approx 1.001$$

With  $x_0$  as 2.1 chord lengths forward of the airfoil, and  $x_1$  as 2.0, the corresponding magnitudes of air-velocity components are  $u_{x_0}=0.9979$  and  $u_{x_1}=0.9978$ . The value of  $\Delta x$  is then 0.1, and the value of  $B$  is 17.228, from which the value of  $v_{x_1}$  from equation (A5) is 0.9979. Therefore, the initial assumption of  $-(v_{x_1}-u_{x_1})=0.0001$  was very nearly correct.

Since the quantity  $(v_{y_1}-u_{y_1})^2$  contributes very little to the initial value of  $C_D R/24$ , once the approximate value of  $v_{x_1}-u_{x_1}$  has been determined, an approximation of  $v_{y_1}-u_{y_1}$  may be made by equation (A6) without changing the initial value chosen for  $C_D R/24$ . For the trajectory calculated in table II,  $v_{y_1}-u_{y_1}$  was assumed to be  $0.1 \times 10^{-5}$ , and it was also found by equation (A2) and (A6) to be of this magnitude.

After the differentials  $v_{x_1}-u_{x_1}$  and  $v_{y_1}-u_{y_1}$  are evaluated, they are entered in the appropriate columns in table II, and the process continued by the steps indicated in the table.

## REFERENCES

1. Kantrowitz, Arthur: Aerodynamic Heating and the Deflection of Drops by an Obstacle in an Air Stream in Relation to Aircraft Icing. NACA TN No. 779, 1940.
2. Glauert, Muriel: A Method of Constructing the Paths of Raindrops of Different Diameters Moving in the Neighbourhood of (1) a Circular Cylinder, (2) an Aerofoil, Placed in a Uniform Stream of Air; and a Determination of the Rate of Deposit of the Drops on the Surface and the Percentage of Drops Caught. R.&M. No. 2025, British A.R.C., 1940.
3. Langmuir, Irving, and Blodgett, Katherine B.: A Mathematical Investigation of Water Droplet Trajectories. General Electric Rep., July 1945 (Available from Department of Commerce Publications Board as PB No 27565.)
4. Glauert, H : The Elements of Aerofoil and Airscrew Theory Cambridge, The University Press, 1926
5. Lewis, William: A Flight Investigation of the Meteorological Conditions Conducive to the Formation of Ice on Airplanes NACA TN No. 1393, 1947.
6. Pierce, B. C : A Short Table of Integrals. Ginn and Company, 1929.

TABLE I

VALUES OF  $\frac{C_D R}{24}$  AS FUNCTIONS OF R

R	$\frac{C_D R}{24}$	R	$\frac{C_D R}{24}$
0.00	1.00	200	6.52
.05	1.009	250	7.38
.1	1.013	300	8.26
.2	1.037	350	9.00
.4	1.073	400	9.82
.6	1.103	500	11.46
.8	1.142	600	12.97
1.0	1.176	800	15.81
1.2	1.201	1000	18.62
1.4	1.225	1200	21.3
1.6	1.248	1400	24.0
1.8	1.267	1600	26.9
2.0	1.285	1800	29.8
2.5	1.332	2000	32.7
3.0	1.374	2500	40.4
3.5	1.412	3000	47.8
4.	1.447	3500	55.6
5.	1.513	4000	63.7
6.	1.572	5000	80.0
8.	1.678	6000	96.8
10.	1.782	8000	130.6
12.	1.901	10000	166.3
14.	2.009	12000	204.
16.	2.109	14000	243.
18.	2.198	16000	285.
20.	2.291	18000	325.
25.	2.489	20000	365.
30.	2.673	25000	470.
35.	2.851	30000	574.
40.	3.013	35000	674.
50.	3.327	40000	778.
60.	3.60	50000	980.
80.	4.11	60000	1175.
100.	4.59	80000	1552.
120.	5.01	10 <sup>5</sup>	1905.
140.	5.40	1.2x10 <sup>5</sup>	2234.
160.	5.76	1.4x10 <sup>5</sup>	2549.
180.	6.16	1.6x10 <sup>5</sup>	2851.

TABLE II.- COMPUTATION OF A WATER-DROP TRAJECTORY  
 $[Ru^2 = 9.15 \times 10^3; K = 0.0581]$

$\Delta t$	$v_{x_n}$	$u_{x_n}$	$\frac{C_{DR}}{24}$	$\frac{C_{DR}}{24K}$	$v_{x_n} - u_{x_n}$	$\frac{C_{DR}}{24K} (v_{x_n} - u_{x_n})$	$\frac{C_{DR}}{24K} (v_{x_n} - u_{x_n}) \Delta t$
0.05	0.9979	0.9978	1.001	17.2289	0.0001	0.001722	0.997814
.05	.9978	.9976	1.002	17.2461	.0002	.002828	.997675
.10	.9977	.9975	1.002	17.2461	.0002	.002983	.997375
.10	.9974	.9972	1.003	17.2633	.0002	.003884	.996987
.10	.9970	.9968	1.003	17.2633	.0002	.003228	.996664
.10	.9967	.9964	1.004	17.2805	.0003	.004562	.996208
.10	.9962	.9960	1.003	17.2633	.0002	.003591	.995849
.10	.9958	.9955	1.006	17.3150	.0003	.006042	.995245
.10	.9952	.9950	1.004	17.2805	.0002	.004233	.994822
.10	.9948	.9944	1.008	17.3494	.0004	.008188	.994003
.10	.9940	.9935	1.009	17.3666	.0005	.008735	.993130
.10	.9931	.9922	1.016	17.4871	.0009	.016263	.991504
.10	.9915	.9910	1.009	17.3666	.0005	.008752	.990629
.10	.9906	.9892	1.024	17.6248	.0014	.025168	.988112
.10	.9881	.9870	1.019	17.5387	.0011	.019503	.986162
.10	.9861	.9840	1.038	17.8657	.0022	.038625	.982299
.10	.9823	.9795	1.050	18.0723	.0028	.050584	.977241
.10	.9772	.9725	1.083	18.6403	.0047	.088373	.968404
.10	.9684	.9610	1.126	19.3804	.0074	.143512	.954053
.10	.9540	.9400	1.220	20.9983	.0141	.295089	.924544
.01	.9245	.8925	1.379	23.7349	.0320	.760561	.916938
.01	.9169	.8845	1.382	23.7866	.0324	.771590	.909222
.01	.9092	.8750	1.396	24.0275	.0342	.822269	.901199
.01	.9011	.8650	1.410	24.2685	.0362	.878495	.892414
.01	.8924	.8530	1.432	24.6472	.0394	.971445	.882700
.01	.8827	.8380	1.468	25.2668	.0447	1.12943	.871406
.01	.8714	.8220	1.498	25.7831	.0494	1.27384	.858668
.01	.8587	.8020	1.544	26.5749	.0567	1.50595	.843609
.01	.8436	.7790	1.588	27.3322	.0647	1.76591	.825950
.01	.8260	.7510	1.648	28.3649	.0750	1.97605	.806190
.01	.8062	.7140	1.738	29.9139	.0922	2.75776	.778612
.01	.7786	.6680	1.870	32.1859	.1106	3.56015	.743011
.01	.7430	.6110	1.990	34.2513	.1320	4.52155	.697796
.01	.6978	.5420	2.180	37.5215	.1558	5.84570	.639339
.01	.6393	.4720	2.350	40.4475	.1673	6.76844	.571655
.01	.5717	.4400	2.600	44.7504	.1317	5.89161	.512739
.01	.5127	.5440	2.536	43.6489	-.0413	1.80100	.530749
.01	.5307	.7000	2.540	43.7177	-.1693	7.39926	.504742

TABLE II.- CONTINUED. COMPUTATION OF A WATER-DROP TRAJECTORY  
 $[R_0^2 = 9.15 \times 10^8; K = 0.0581]$

$\Delta V_{x_n}$	$\Delta t$	$\frac{C_{DR}}{24K} \left( \frac{v_{x_n} - u_{x_n}}{2} \right)$	$\frac{C_{DR}}{24K} \left( \frac{v_{x_n} - u_{x_n}}{2} \right) \times \Delta t^2 \times 10^{-18}$	$\frac{C_{DR}}{24K} \left( \frac{v_{x_n} - u_{x_n}}{2} \right) \times \Delta t$	$\frac{v}{c}$	$v_{y_n} \times 10^{-18}$	$u_{y_n} \times 10^{-18}$
0.049895	0.0025	0.00086	2.1500	0.049895	1.95011	1.5000	1.60
.049890	.0025	.00141	3.5350	.049887	1.90022	1.5861	1.75
.0997673	.0100	.00150	14.9179	.099752	1.80047	1.7274	1.90
.0997375	.0100	.00194	19.4212	.099718	1.70075	2.0250	2.20
.0996987	.0100	.00161	16.1412	.099674	1.60108	2.3270	2.50
.0996664	.0100	.00228	22.8102	.099644	1.50144	2.6258	2.90
.0996208	.0100	.00180	17.9569	.099603	1.40184	3.0997	3.50
.0995849	.0100	.00302	30.2147	.099555	1.30229	3.7941	4.20
.0995245	.0100	.00211	21.1686	.099503	1.20279	4.4969	5.0
.0994822	.0100	.00409	40.9446	.099441	1.10335	5.3662	6.0
.0994003	.0100	.00456	43.6770	.099357	1.00399	6.4657	7.4
.0993130	.0100	.00813	81.3150	.099232	.90476	8.0862	9.2
.0991504	.0100	.00457	43.7638	.099107	.80565	10.032	12.0
.0990829	.0100	.01258	125.841	.098937	.70671	13.452	15.5
.0988112	.0100	.00975	97.515	.098714	.60800	17.061	20.0
.0986162	.0100	.01931	193.128	.098423	.50958	22.215	29.0
.0982299	.0100	.02529	252.922	.097977	.41160	34.333	43.0
.0977241	.0100	.04419	441.868	.097282	.31432	49.995	70.0
.0968404	.0100	.07176	717.560	.096123	.21820	87.284	120.0
.0954053	.0100	.14754	1475.44	.093930	.12427	150.689	255.0
.0092454	.0001	.38028	38.0280	.0092074	.11506	369.724	660.0
.0091693	.0001	.38580	38.5795	.0091308	.10593	438.621	750.0
.0090922	.0001	.41113	41.1134	.0090531	.09688	512.687	880.0
.0090119	.0001	.43924	43.9247	.0089680	.08791	600.934	1020.0
.0089241	.0001	.48572	48.5722	.0088755	.07903	702.635	1200.0
.0088270	.0001	.56471	56.4710	.0087705	.07026	825.222	1500.0
.0087140	.0001	.63692	63.6920	.0086503	.06161	995.717	1800.0
.0085866	.0001	.75297	75.2970	.00851138	.05310	1203.09	2300.0
.0084360	.0001	.88295	88.2950	.0083478	.04475	1454.59	2800.0
.0082595	.0001	.98802	98.8020	.0081607	.03659	1862.32	3800.0
.0080619	.0001	1.37888	137.888	.00802301	.02857	2411.94	4800.0
.0077861	.0001	1.78007	178.007	.00760812	.02096	3126.50	7000.0
.0074301	.0001	2.26077	226.077	.00720403	.01376	4373.08	10000.0
.0069779	.0001	2.92285	292.285	.00668568	.00707	6300.37	16000.0
.0063933	.0001	2.38422	338.422	.00605497	.00102	9939.82	25000.0
.0057165	.0001	2.94580	294.580	.00542197	-.00440	16031.3	42500.0
.0051273	.0001	.90050	90.050	.00503734	-.00944	27786.8	55000.0
.0053074	.0001	3.69963	369.963	.00493753	-.01438	39665.1	61700.0

TABLE II.- CONTINUED. COMPUTATION OF A WATER-DROP TRAJECTORY  
 [  $Ru^2 = 9.15 \times 10^3$ ;  $K = 0.0581$  ]

$[v_{yn} - u_{yn}] \times 10^{+5}$	$\frac{C_{DR}}{24K} (v_{yn} - u_{yn}) \times 10^{+5}$	$\left[ \frac{C_{DR}}{24K} (v_{xn} - u_{xn}) \Delta t \right] \times 10^{+5}$	$v_{yn} \Delta t \times 10^{+5}$	$\left[ \frac{C_{DR}}{24K} (v_{yn} - u_{yn}) \Delta t^2 \right] \times 10^{+7}$	$y/c \times 10^{+4}$	$\frac{y}{x}$	$Ru$
.10000	1.72289	1.58614	.075	8	75.608	.003877	95.65
.16386	2.82594	1.72744	.079	8	75.616	.003979	95.65
.17256	2.97599	2.02504	.172	19	75.635	.004200	95.65
.17496	3.02038	2.32708	.202	22	75.657	.004448	95.65
.17292	2.98517	2.62560	.232	25	75.682	.004727	95.65
.27440	4.74177	3.09978	.262	29	75.711	.005043	95.65
.40220	6.94330	3.79411	.309	34	75.745	.005403	95.65
.40589	7.02799	4.49691	.379	41	75.786	.005819	95.65
.50309	8.69366	5.36628	.449	49	75.835	.006305	95.65
.63372	10.9947	6.46675	.536	59	75.894	.006878	95.65
.93425	16.2247	8.08822	.646	73	75.967	.007566	95.65
1.11178	19.4418	10.0324	.808	91	76.058	.008406	95.65
1.9676	34.2044	13.4528	1.003	117	76.175	.009455	95.65
2.0472	36.0815	17.0610	1.345	153	76.328	.01080	95.65
2.9390	51.5462	22.2156	1.706	196	76.524	.01259	95.65
6.7844	121.208	34.3334	2.221	283	76.807	.01507	95.65
8.6666	156.625	49.9959	3.433	422	77.229	.01876	95.65
20.0041	372.982	87.2841	4.999	681	77.910	.02479	95.65
32.7159	654.047	150.689	8.728	1190	79.100	.03625	95.65
104.311	2190.35	369.724	15.068	2602	81.702	.065715	95.65
290.276	6889.67	438.621	3.697	404	82.106	.07136	95.65
311.379	7406.65	512.687	4.386	476	82.582	.07796	95.65
367.313	8825.61	600.934	5.126	557	83.139	.08582	95.65
419.066	101.701 $\times 10^2$	702.635	6.009	652	83.791	.09531	95.65
497.365	122.587 $\times 10^2$	825.222	7.026	764	84.555	.1070	95.65
674.778	170.495 $\times 10^2$	995.717	8.252	910	85.465	.1216	95.65
804.283	207.369 $\times 10^2$	1203.09	9.957	1099	86.564	.1405	95.65
1096.910	291.503 $\times 10^2$	1494.59	12.030	1349	87.913	.1655	95.65
1345.410	367.730 $\times 10^2$	1862.32	14.545	1638	89.551	.2001	95.65
1937.68	549.621 $\times 10^2$	2411.94	18.623	2137	91.688	.2506	95.65
2388.06	714.362 $\times 10^2$	3126.30	24.119	2769	94.457	.3306	95.65
3673.70	124.679 $\times 10^3$	4373.08	31.263	3750	98.207	.4685	95.65
5626.92	192.729 $\times 10^3$	6300.37	43.730	5337	103.544	.8110	95.65
9699.63	363.945 $\times 10^3$	9939.82	63.003	8120	111.664	1.5941	95.65
15060.0	609.147 $\times 10^3$	16031.3	99.398	12986	124.650	12.450	95.65
26269.2	1175.548 $\times 10^3$	27786.8	160.313	21909	146.559	3.3320	95.65
27213.2	1187.826 $\times 10^3$	39665.1	277.868	33726	180.285	1.9100	95.65
22034.9	963.316 $\times 10^3$	49298.3	396.651	44482	---	---	---



TABLE II.- CONTINUED. COMPUTATION OF A WATER-DROP TRAJECTORY  
 [  $R_0 = 9.15 \times 10^3$ ;  $K = 0.0681$  ]

$r_{n+1}$	$u_{n+1} \times 10^4$	$\frac{CDR}{24K} (v_{n+1}^2 - v_n^2) \Delta t$	$[\frac{CDR}{24K} (v_{n+1}^2 - v_n^2) \Delta t] u_{n+1} \times 10^4$	$[\frac{CDR}{24K} (v_{n+1}^2 - v_n^2) \Delta t] u_{n+1}^2 \times 10^8$	$[\frac{CDR}{24K} (v_{n+1}^2 - v_n^2) \Delta t] u_{n+1}^3 \times 10^{12}$	$\frac{r}{R_0}$	$R$
0.99765	1.76	0.000164	0.16386	2.6896	2.68501	0.000164	0.01668
0.99750	1.90	0.000173	0.17286	2.9929	2.97770	0.000173	0.01655
0.99713	2.20	0.000225	0.17496	5.0625	3.06110	0.000225	0.02152
0.9968	2.50	0.000187	0.17292	3.4969	2.99013	0.000187	0.01788
0.9964	2.90	0.000264	0.27440	6.9696	7.5295	0.000264	0.02525
0.9960	3.50	0.000209	0.40220	4.3264	16.1765	0.000209	0.01990
0.9955	4.20	0.000349	0.40889	12.1801	16.4747	0.000349	0.03338
0.9950	5.00	0.000245	0.50509	6.0025	25.3100	0.000245	0.02343
0.9944	6.00	0.000472	0.53372	22.2784	40.1601	0.000472	0.04515
0.9935	7.40	0.000503	0.93425	25.5009	87.2825	0.000503	0.04811
0.9922	9.20	0.000930	1.11178	86.4900	125.605	0.000930	0.08895
0.9910	12.0	0.000504	1.99776	25.5016	387.145	0.00504	0.06821
0.9892	15.5	0.001428	2.0472	203.918	419.103	0.003428	0.1565
0.9870	20.0	0.001112	2.8390	123.650	863.772	0.001112	0.1064
0.9840	29.0	0.002162	6.7844	467.424	4602.81	0.002165	0.2069
0.9795	43.0	0.002799	8.6656	783.44	7510.48	0.002800	0.2678
0.9725	70.0	0.004741	20.0041	2247.71	40016.0	0.004745	0.4538
0.9610	120.0	0.007404	32.7159	5481.92	101.033x10 <sup>4</sup>	0.007411	0.798
0.9400	255.0	0.014053	104.511	19748.7	1081.070x10 <sup>4</sup>	0.014092	1.5479
0.925	660.0	0.032044	290.276	10268.2	8426.000x10 <sup>4</sup>	0.032175	3.0775
0.8925	780.0	0.032438	311.379	10522.2	9695.690x10 <sup>4</sup>	0.032597	3.1169
0.8645	880.0	0.034222	367.315	117115.0	1349.190x10 <sup>4</sup>	0.034418	3.2921
0.8650	1020.0	0.036199	419.066	131037.0	1766.160x10 <sup>4</sup>	0.036440	3.4855
0.8550	1200.0	0.039414	497.365	155346.0	2473.720x10 <sup>4</sup>	0.039726	3.7998
0.8380	1500.0	0.044700	674.778	199809.0	4553.250x10 <sup>4</sup>	0.045206	4.3240
0.8200	1800.0	0.049406	804.283	244095.0	6165.710x10 <sup>4</sup>	0.050066	4.7879
0.8020	2300.0	0.058668	1096.91	321126.0	120.321x10 <sup>4</sup>	0.05772	5.5309
0.7790	2800.0	0.064609	1345.41	417432.0	181.013x10 <sup>4</sup>	0.0659	6.3119
0.7510	3800.0	0.074950	1937.68	561750.0	375.460x10 <sup>4</sup>	0.07741	7.4083
0.7140	4800.0	0.082190	2388.06	849899.0	570.283x10 <sup>4</sup>	0.08523	9.1090
0.6650	7000.0	0.110612	2873.70	1223500.	150.055x10 <sup>4</sup>	0.1172	11.2101
0.6110	10000.0	0.132011	5636.82	1742690.	316.622x10 <sup>4</sup>	0.1435	13.7288
0.5420	16000.0	0.167339	9699.63	2427240.	940.828x10 <sup>4</sup>	0.1835	17.6508
0.4720	26000.0	0.167339	15060.2	2800230.	226.809x10 <sup>4</sup>	0.2251	21.5518
0.4400	42300.0	0.131665	26269.0	1733300.	690.060x10 <sup>4</sup>	0.2938	28.1020
0.5540	55000.0	0.041261	27213.2	170247.	740.558x10 <sup>4</sup>	0.2752	26.5367
0.7000	61700.0	0.169251	22034.9	2864590.	485.537x10 <sup>4</sup>	0.2779	26.5754

NATIONAL ADVISORY  
 COMMITTEE FOR AERONAUTICS

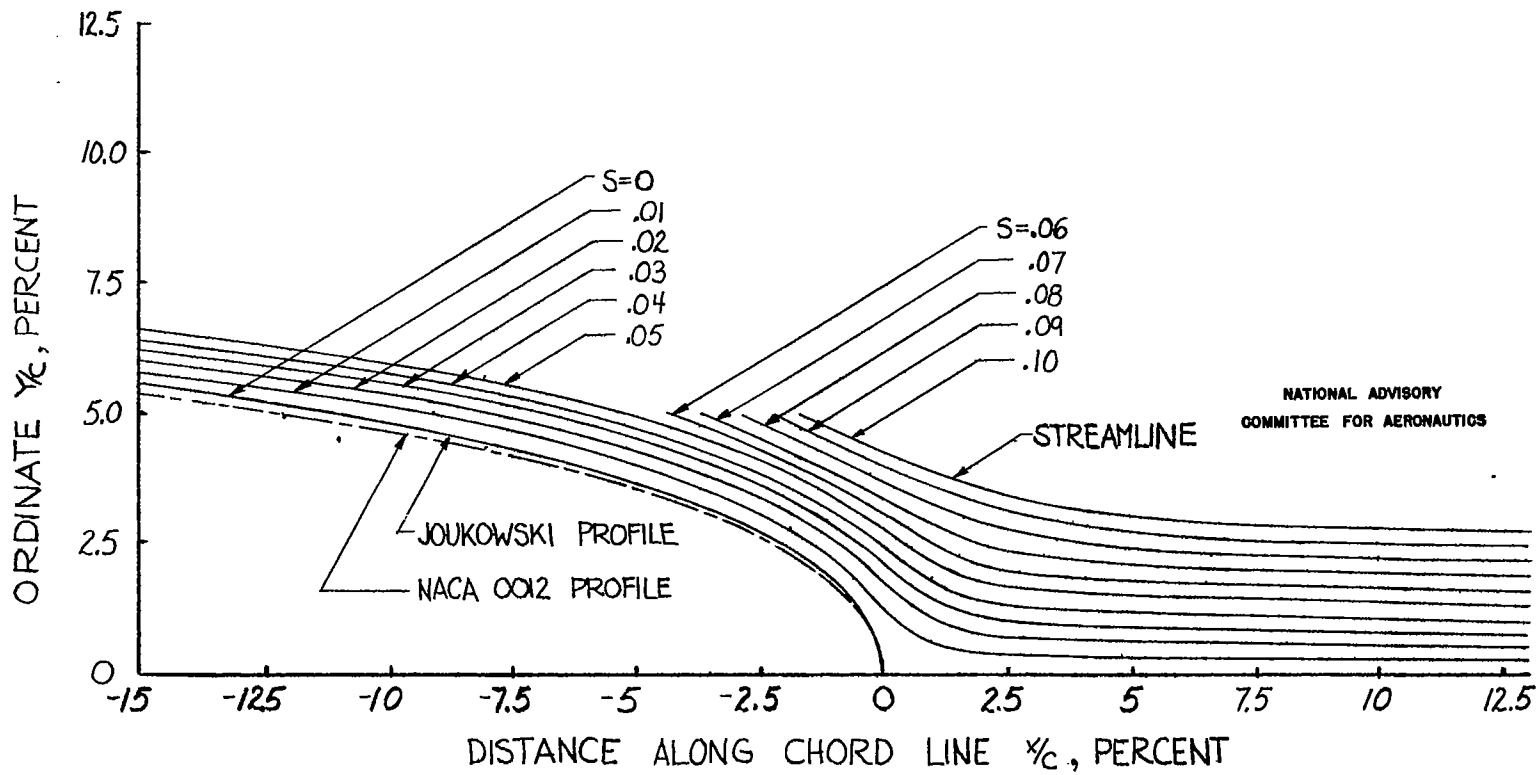
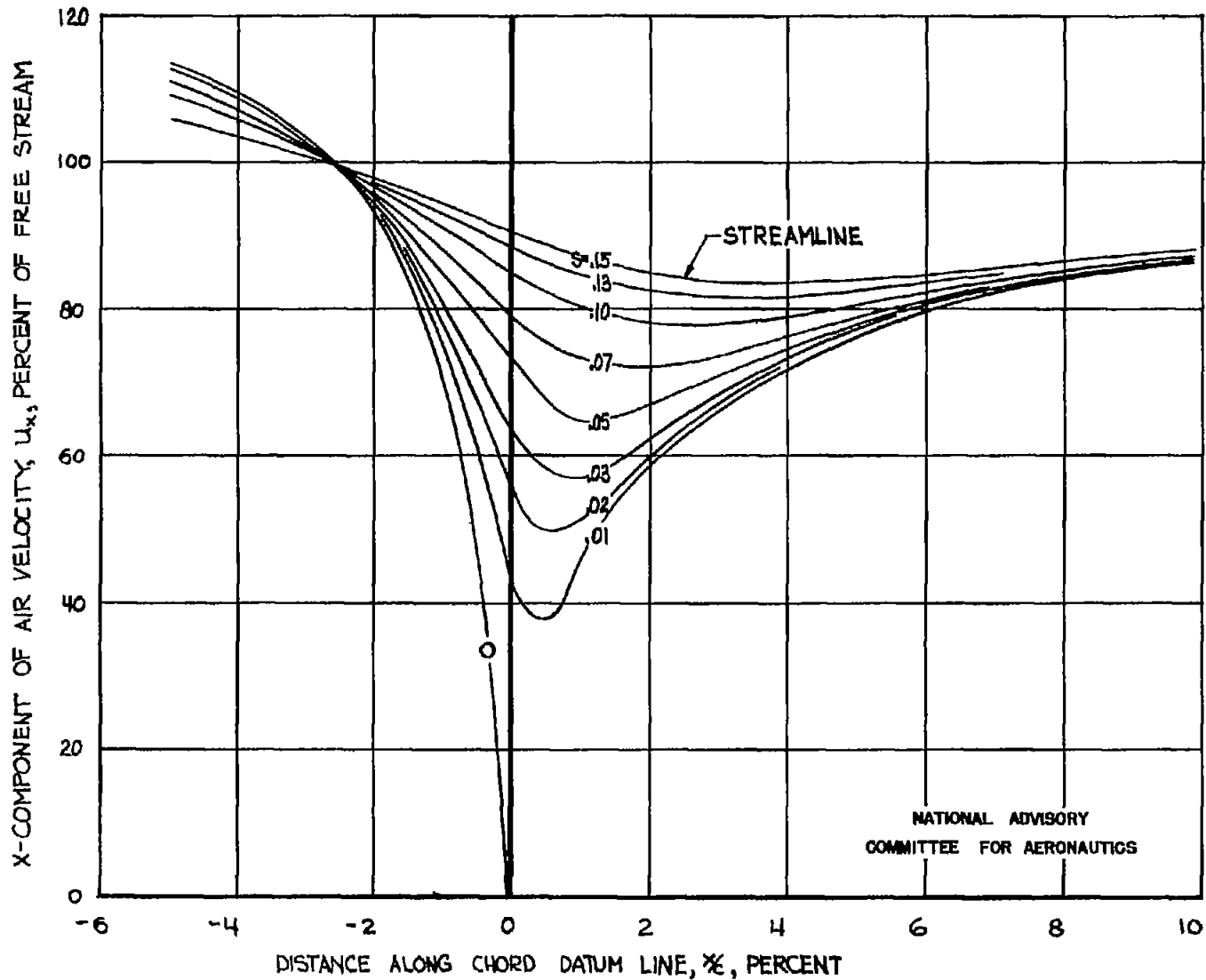


FIGURE 1.- STREAMLINE FIELD ABOUT A SYMMETRICAL JOUKOWSKI AIRFOIL 12 PERCENT THICK SHOWING A COMPARISON BETWEEN THE SURFACE STREAMLINES FOR AN NACA 0012 AND THE JOUKOWSKI AIRFOIL



NATIONAL ADVISORY  
COMMITTEE FOR AERONAUTICS

FIGURE 2A.-AIR-VELOCITY-COMPONENT PROFILES FOR VARIOUS STREAMLINES ABOUT A SYMMETRICAL JOUKOWSKI AIRFOIL 12 PERCENT THICK. X-VELOCITY COMPONENTS IN PROXIMITY TO THE AIRFOIL

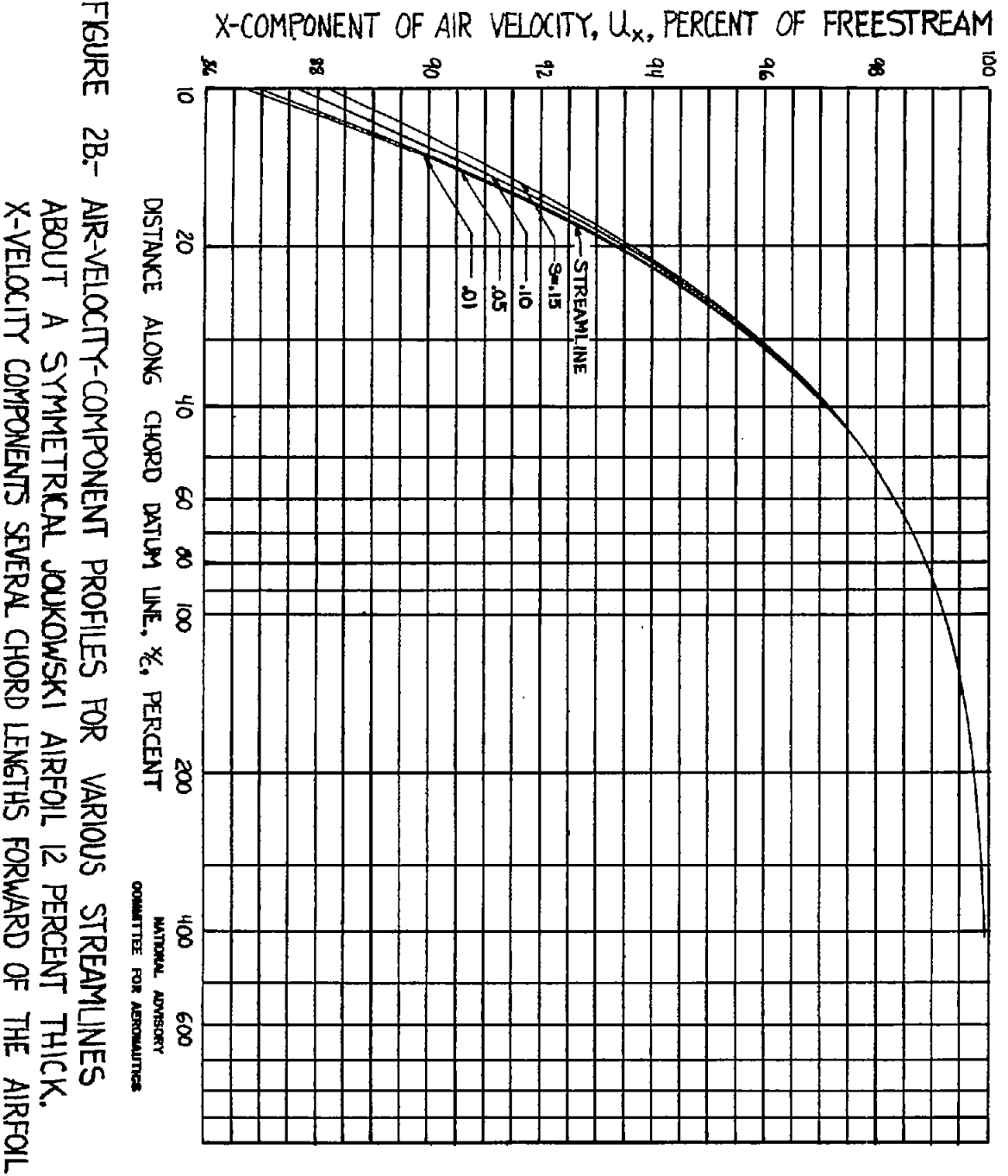
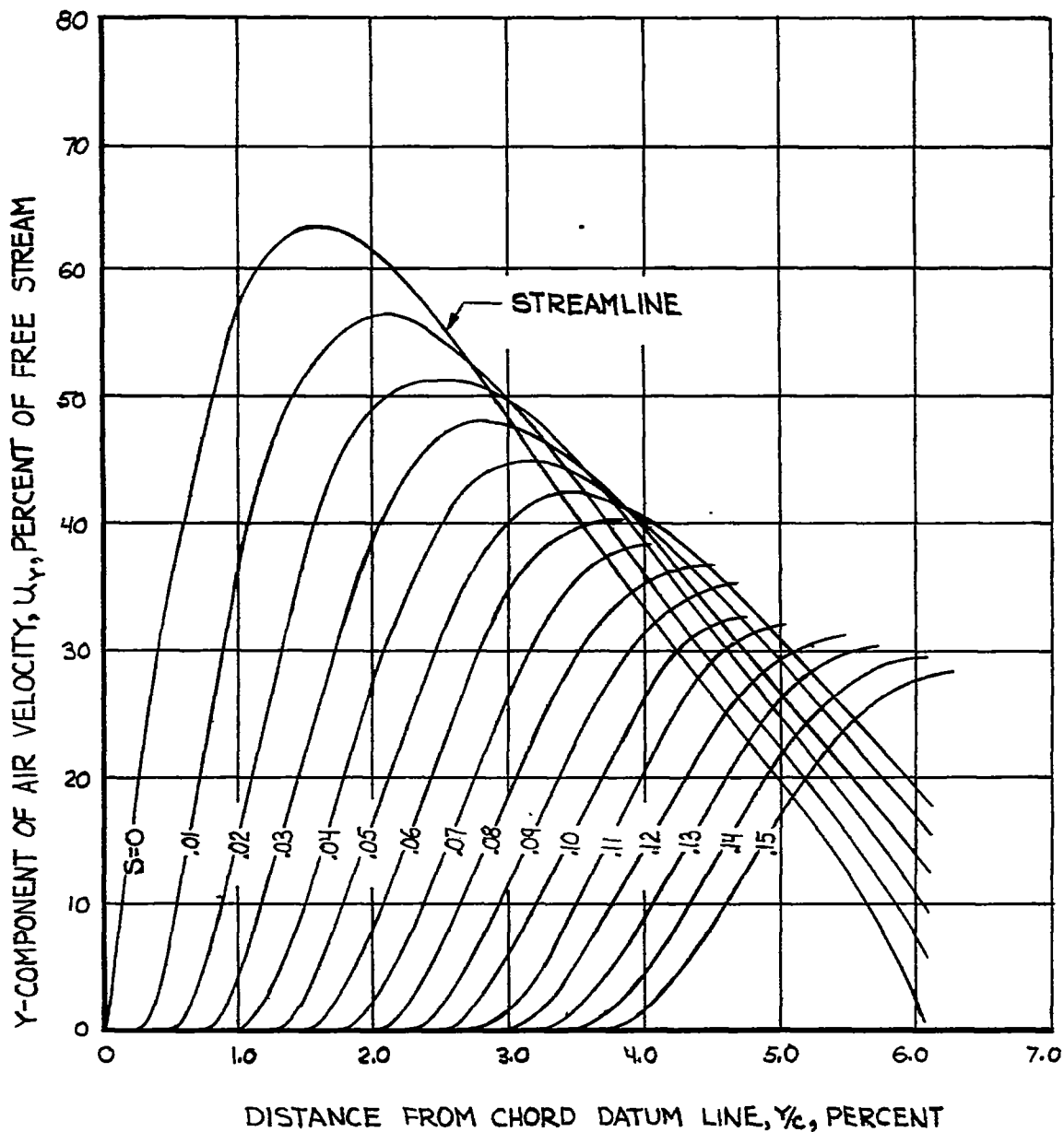


FIGURE 2B.- AIR-VELOCITY-COMPONENT PROFILES FOR VARIOUS STREAMLINES ABOUT A SYMMETRICAL JOUKOWSKI AIRFOIL 12 PERCENT THICK. X-VELOCITY COMPONENTS SEVERAL CHORD LENGTHS FORWARD OF THE AIRFOIL



NATIONAL ADVISORY  
COMMITTEE FOR AERONAUTICS

FIGURE 2C.- AIR-VELOCITY-COMPONENT PROFILES FOR VARIOUS  
STREAMLINES ABOUT A SYMMETRICAL JOUKOWSKI  
AIRFOIL 12 PERCENT THICK. Y-VELOCITY COMPONENTS  
IN PROXIMITY TO THE AIRFOIL

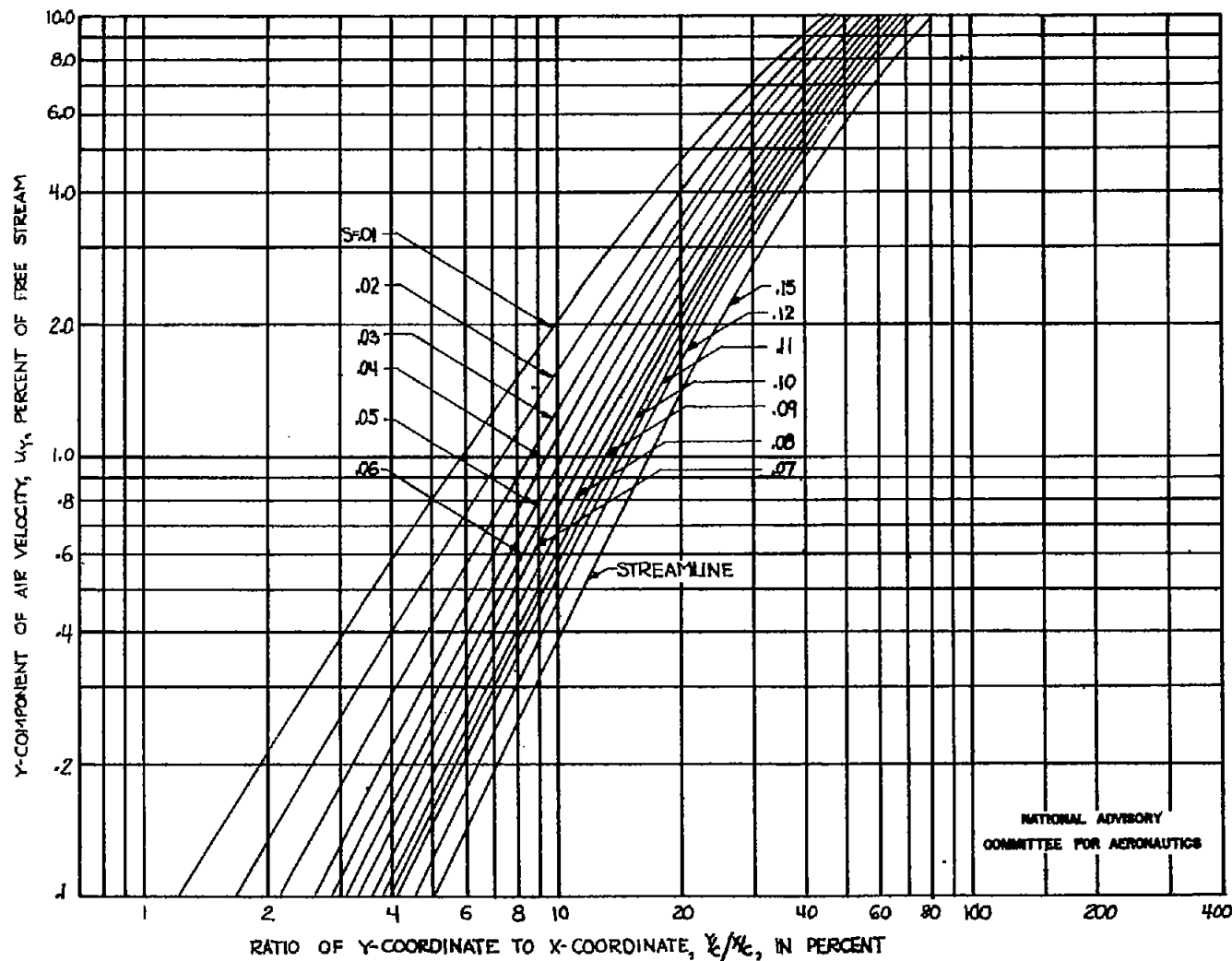


FIGURE 2D.-AIR-VELOCITY COMPONENT PROFILES FOR VARIOUS STREAMLINES ABOUT A SYMMETRICAL JOUKOWSKI AIRFOIL 12 PERCENT THICK. Y-VELOCITY COMPONENTS IN TERMS OF COORDINATE RATIOS

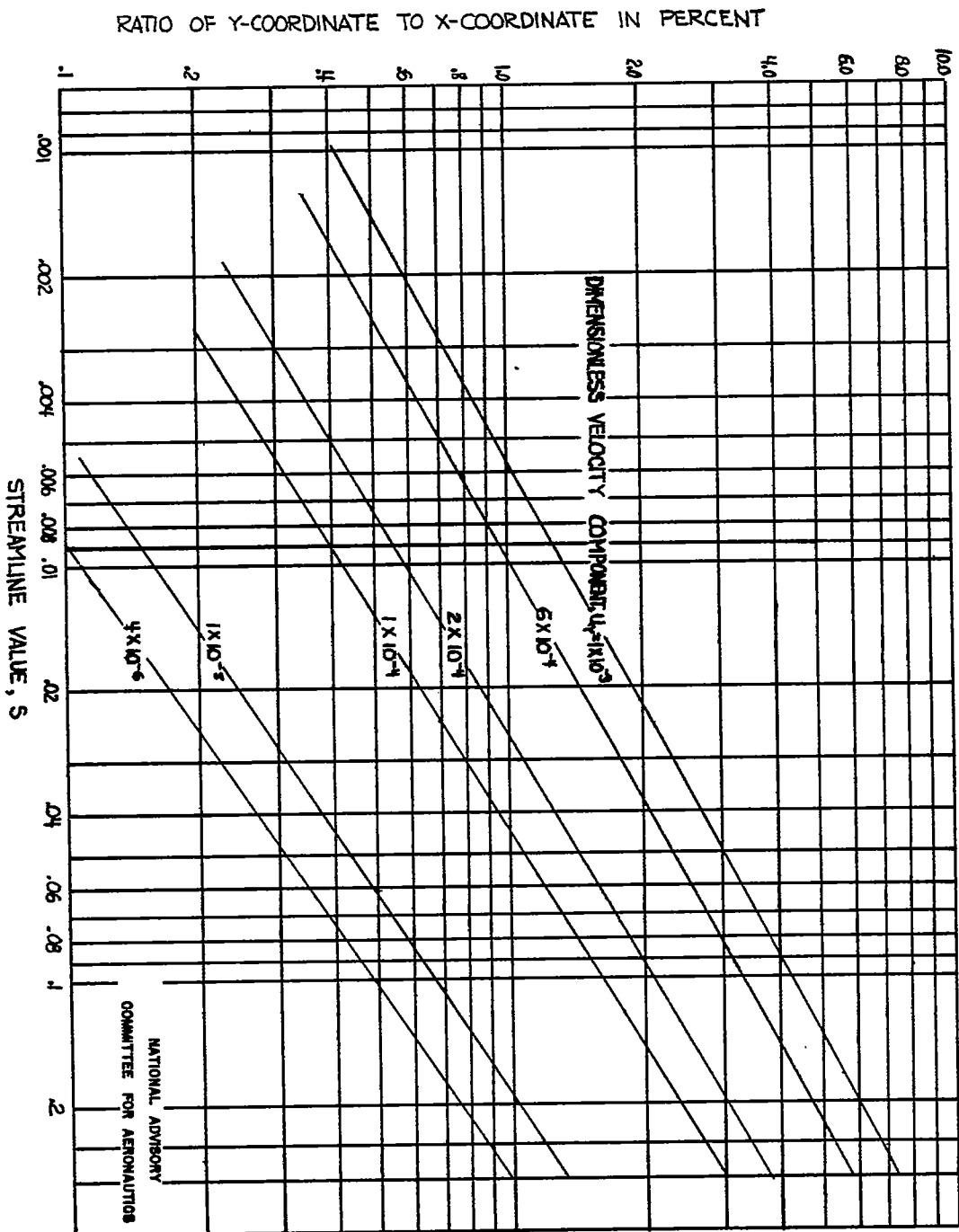


FIGURE 3.- COORDINATE RATIOS OF POINTS ON STREAMLINES AS A FUNCTION OF Y-COMPONENTS OF AIR VELOCITY FOR A SYMMETRICAL DUKOWSKI AIRFOIL 12 PERCENT THICK

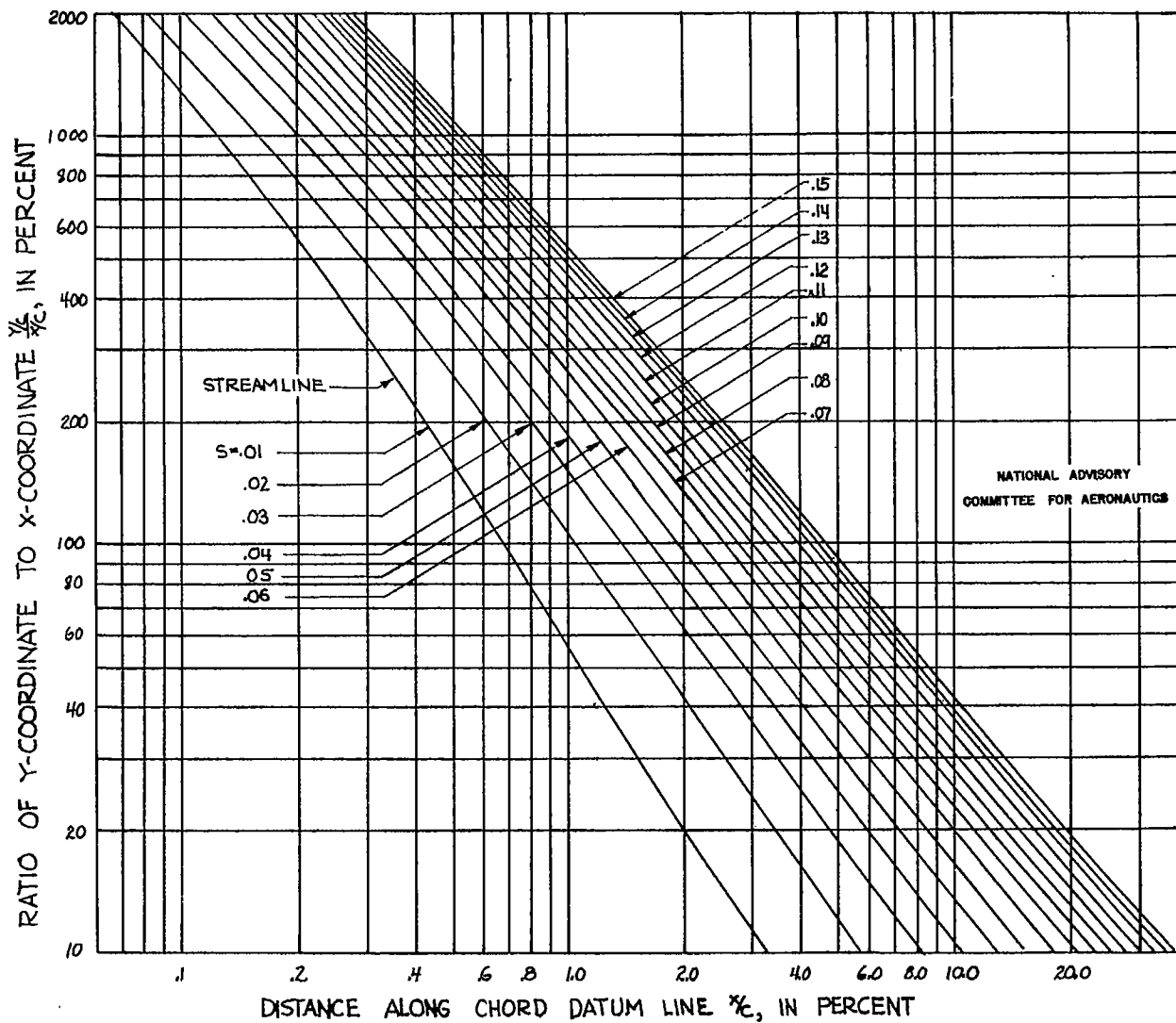


FIGURE 4.- STREAMLINES ABOUT A SYMMETRICAL JOUKOWSKI AIRFOIL 12 PERCENT THICK AS A FUNCTION OF THEIR COORDINATES.



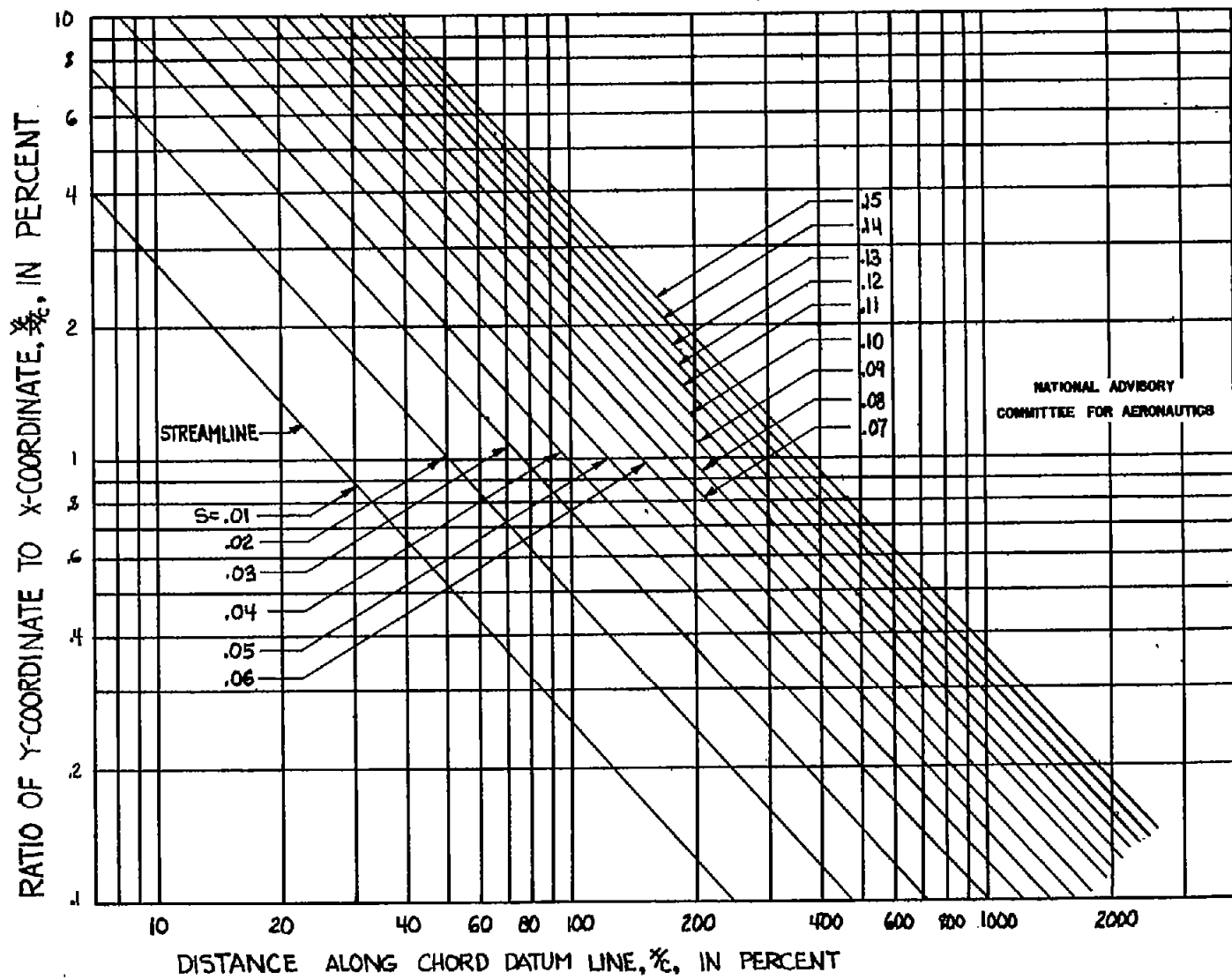


FIGURE 4.-CONCLUDED

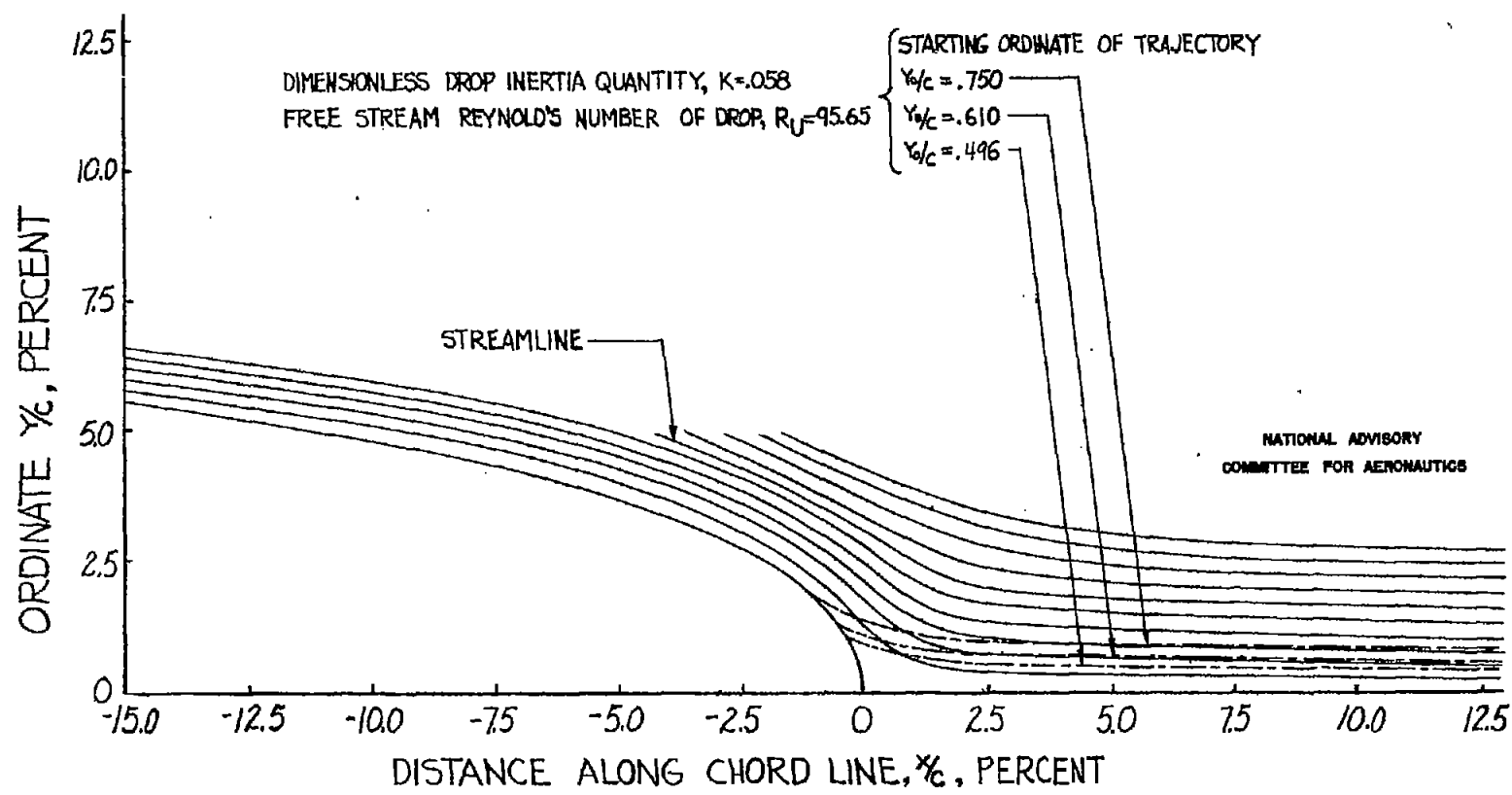


FIGURE 5.- RELATION OF WATER-DROP TRAJECTORIES TO STREAMLINE FIELD ABOUT A SYMMETRICAL JOUKOWSKI AIRFOIL 12 PERCENT THICK.

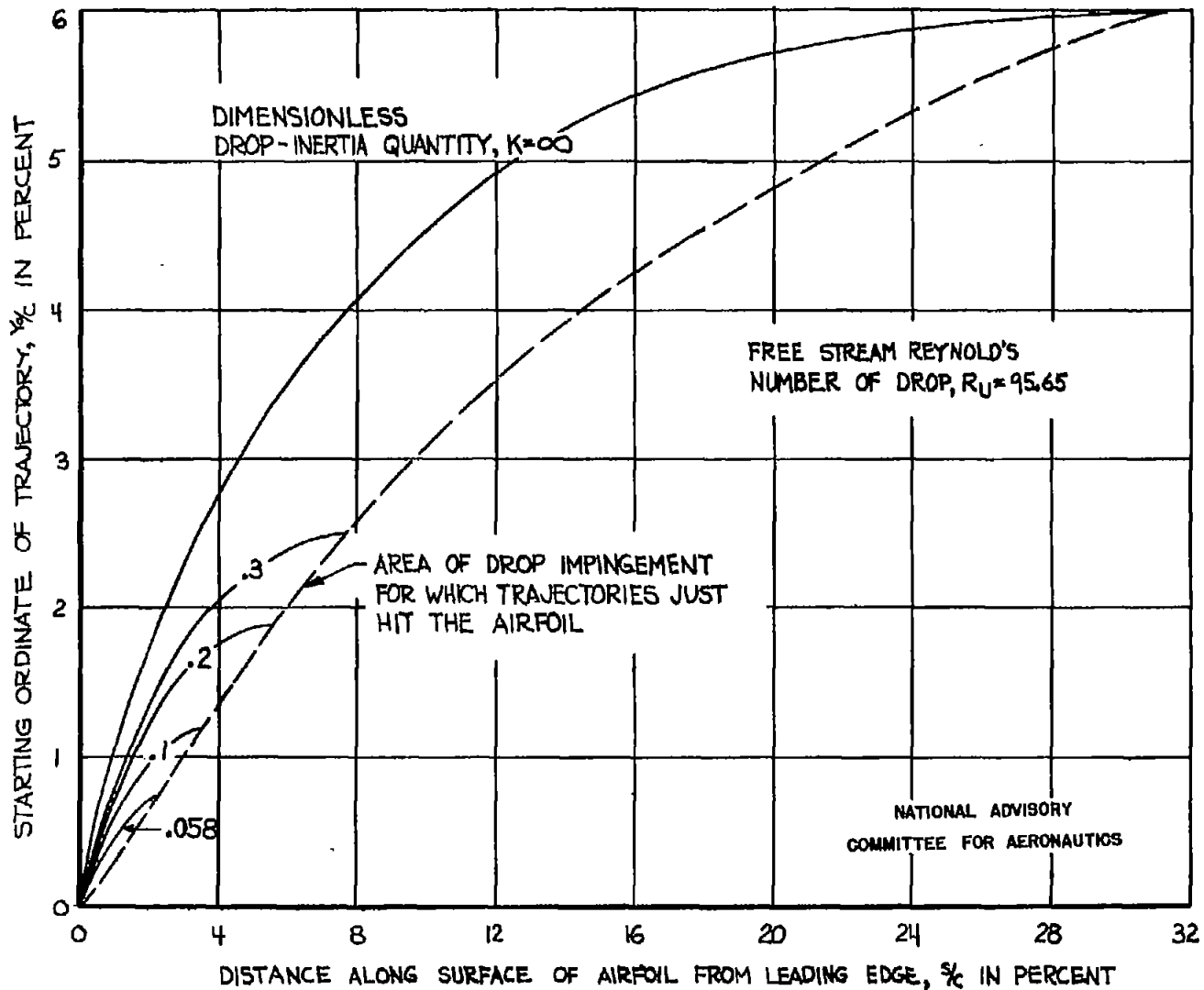


FIGURE 6.- AREA OF DROP INTERCEPTION CORRESPONDING TO DROPS OF DIFFERENT INERTIA FOR A SYMMETRICAL JOUKOWSKI AIRFOIL 12 PERCENT THICK.

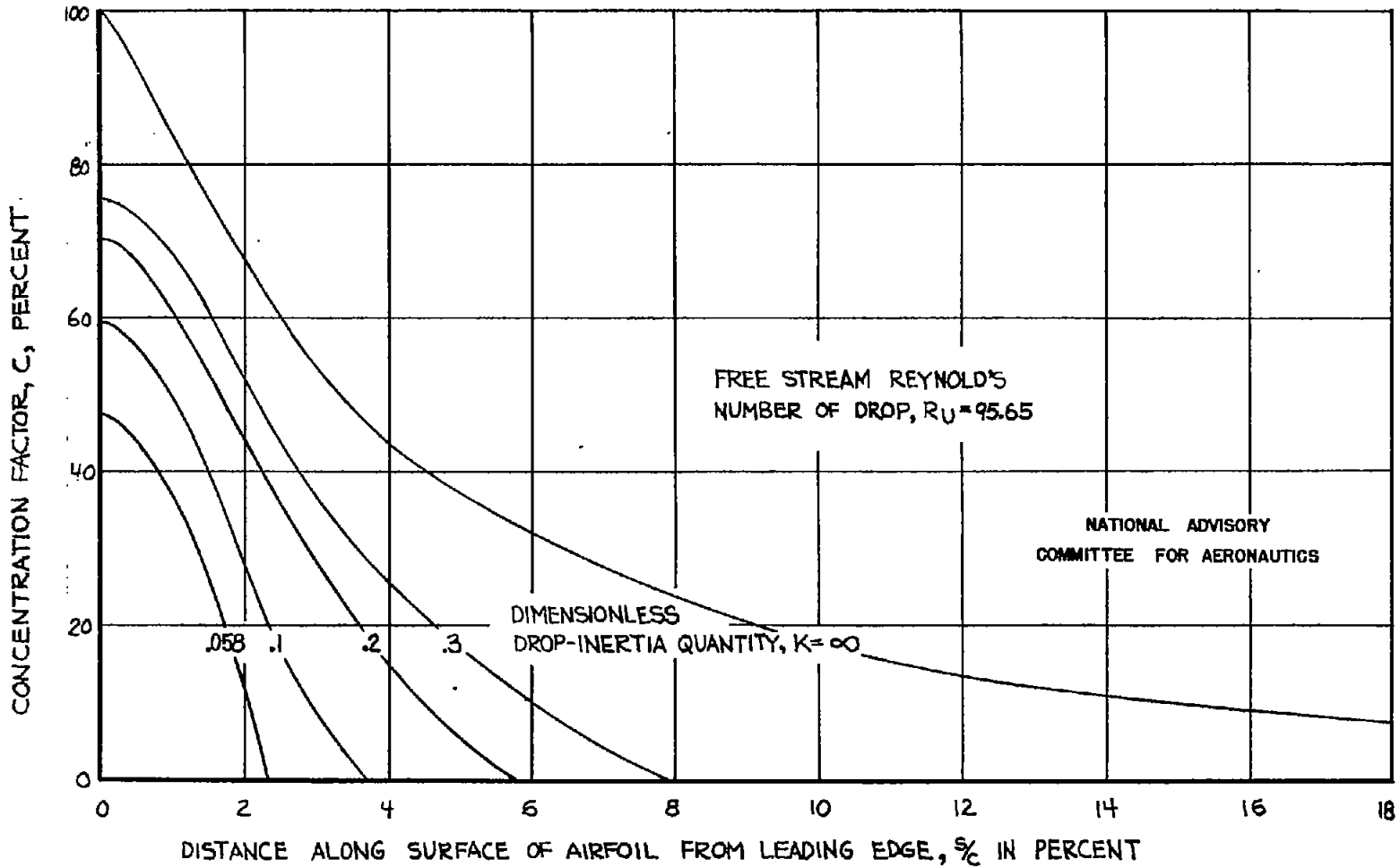


FIGURE 7 - DISTRIBUTION OF WATER-DROP IMPINGEMENT OVER A SYMMETRICAL JOUKOWSKI AIRFOIL 12 PERCENT THICK.

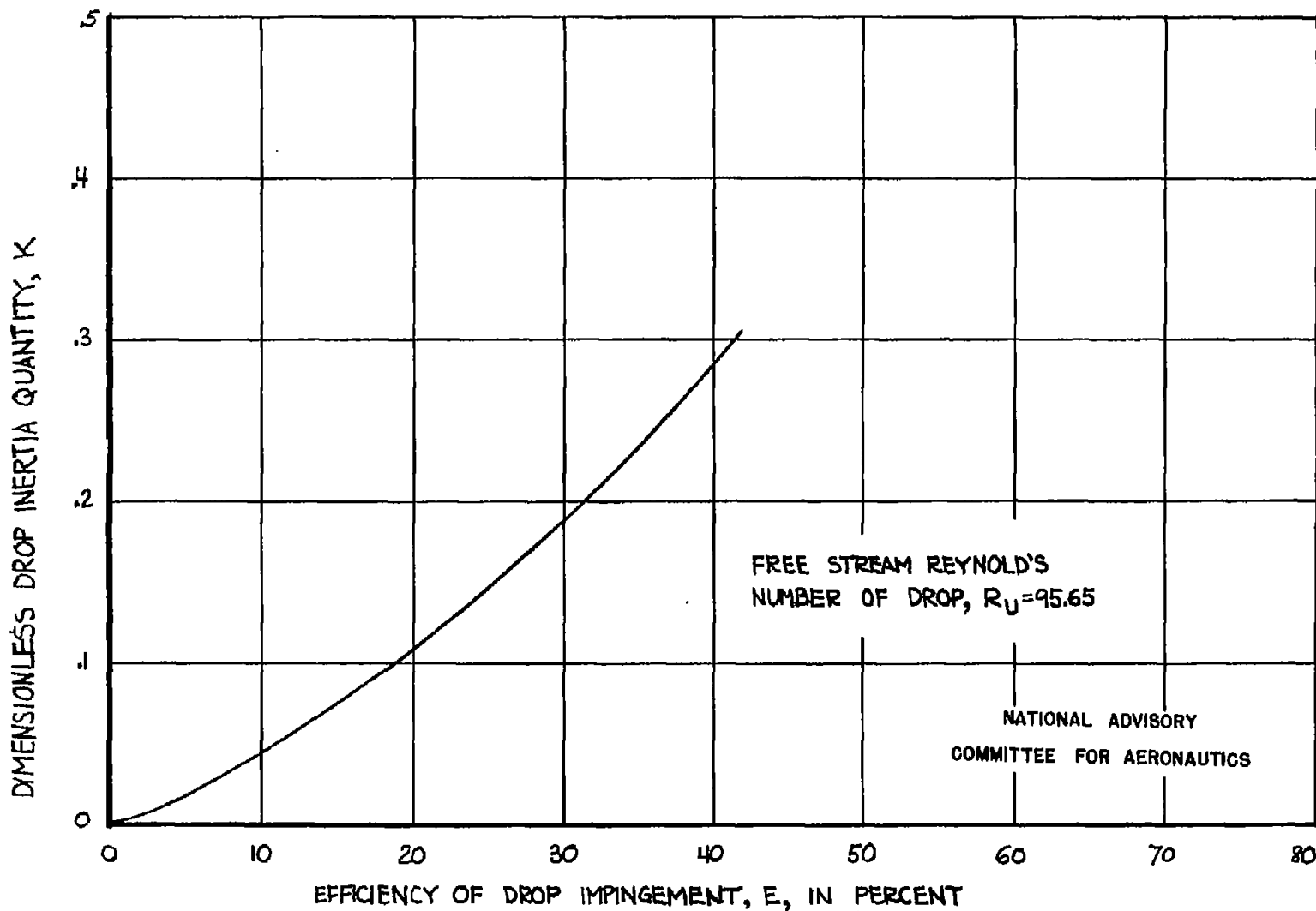


FIGURE 8.- WATER-DROP-COLLECTION EFFICIENCY FOR A SYMMETRICAL JOUKOWSKI AIRFOIL 12 PERCENT THICK.

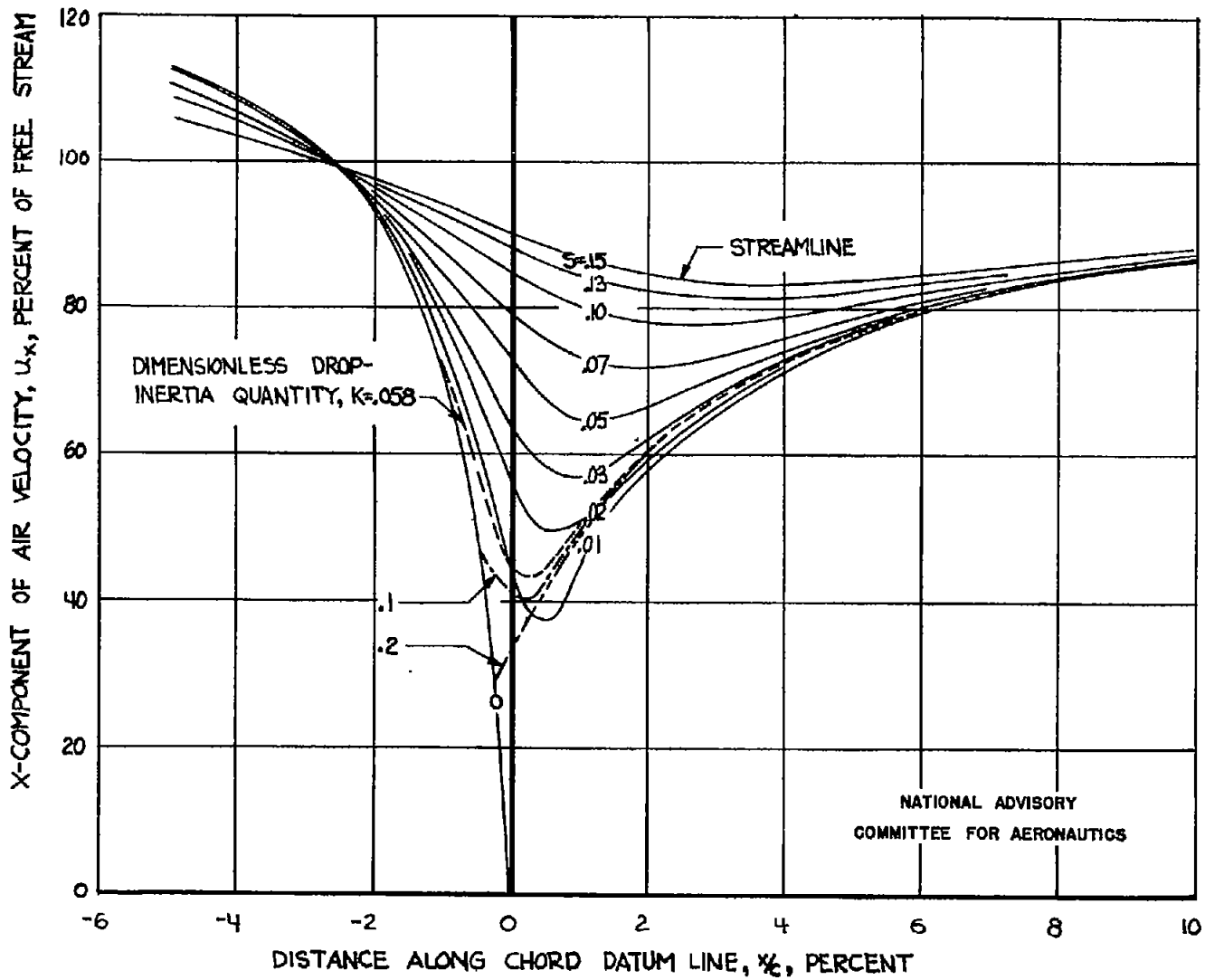
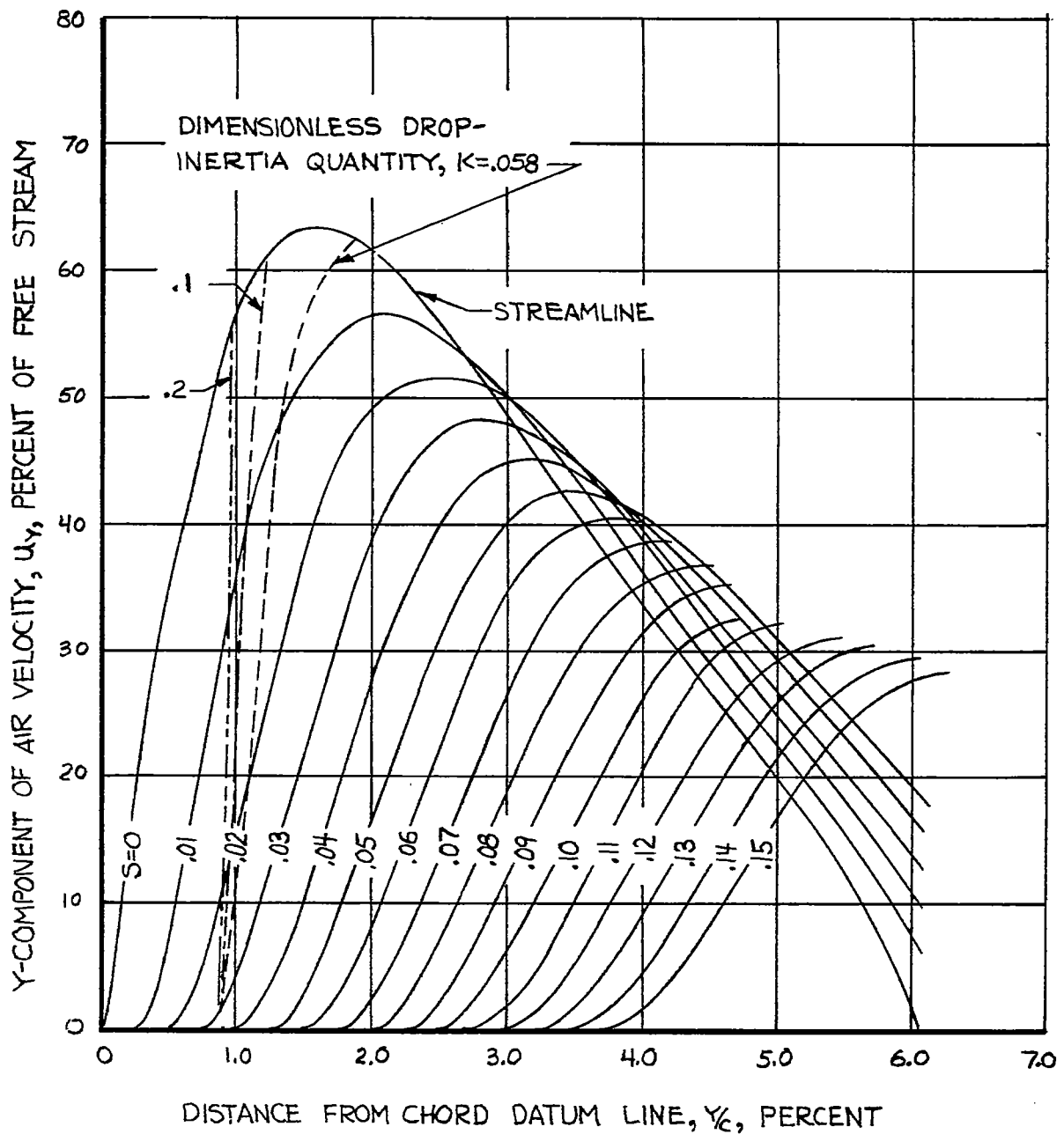


FIGURE 9A- INFLUENCE OF VELOCITY FIELD ON THE PATH OF WATER DROPS HAVING DIFFERENT INERTIA FOR A SYMMETRICAL JOUKOWSKI AIRFOIL 12 PERCENT THICK. X-VELOCITY COMPONENTS



NATIONAL ADVISORY  
COMMITTEE FOR AERONAUTICS

FIGURE 9B.- INFLUENCE OF VELOCITY FIELD ON THE PATH OF WATER DROPS HAVING DIFFERENT INERTIA FOR A SYMMETRICAL JOUKOWSKI AIRFOIL 12 PERCENT THICK. Y-VELOCITY COMPONENTS

FACTOR BY WHICH WATER-DROP IMPINGEMENT IS GREATER  
ON THE AIRFOIL THAN ON THE EQUIVALENT CYLINDER

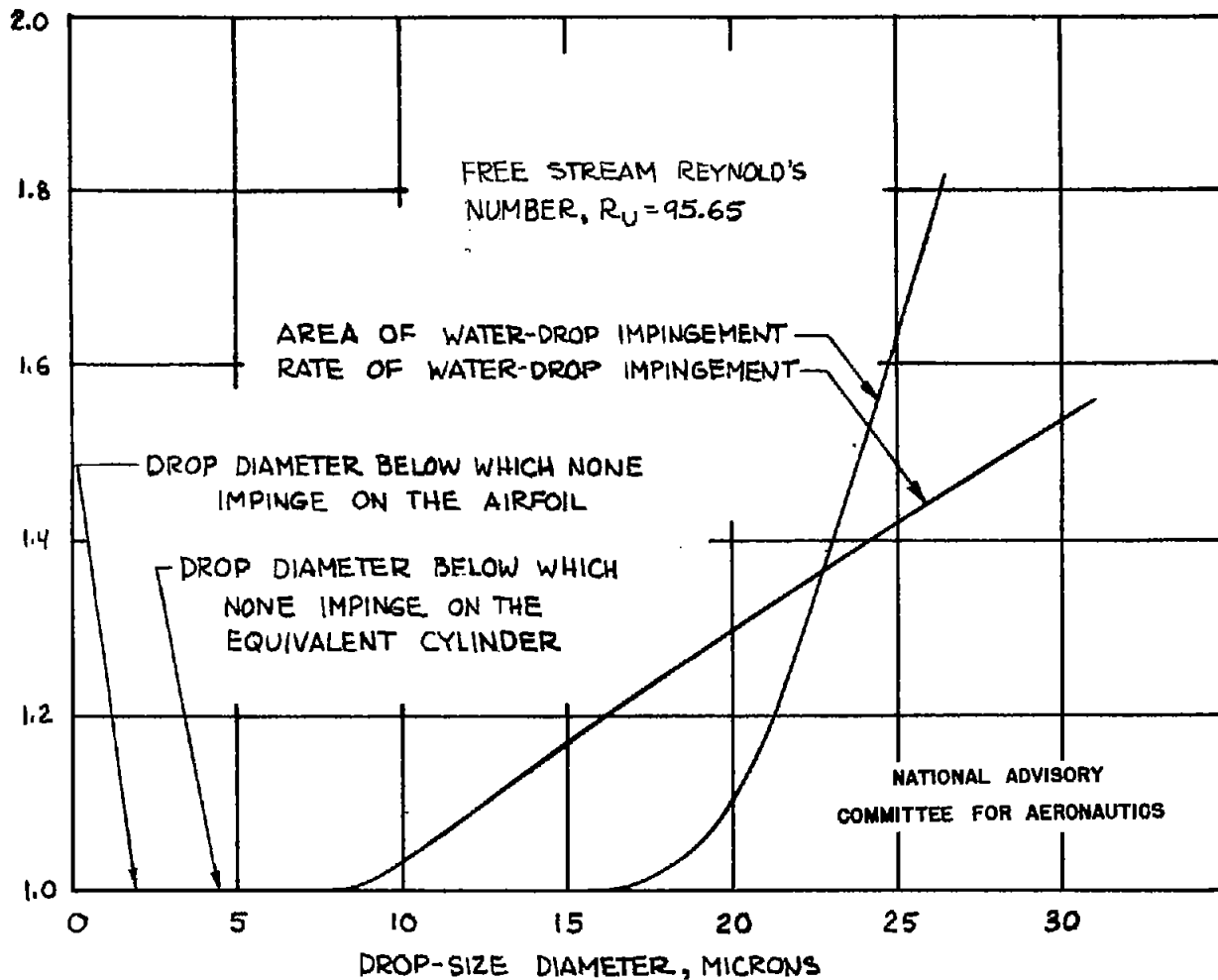
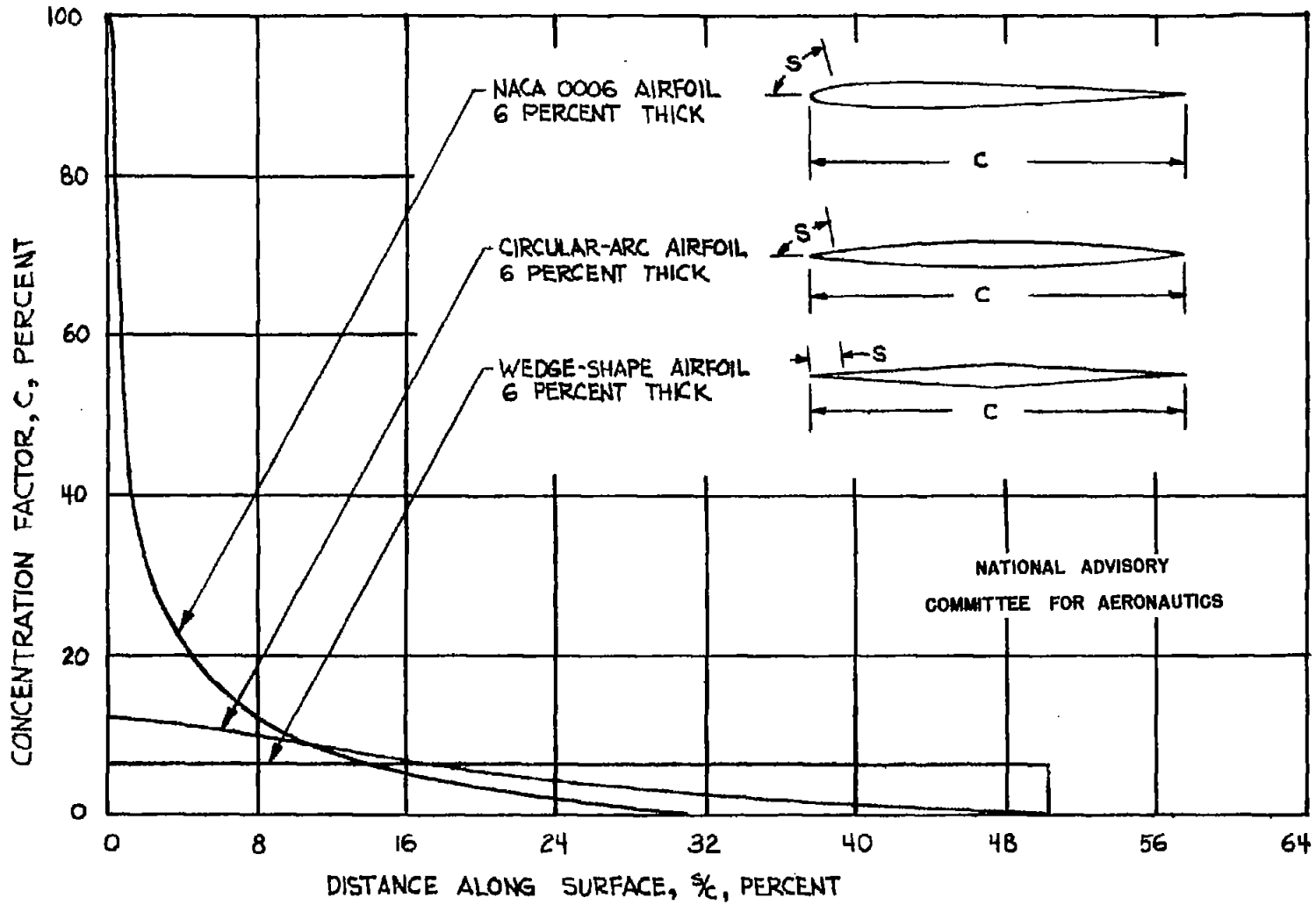


FIGURE 10.- COMPARISON OF RATE AND AREA OF WATER-DROP IMPINGEMENT ON A SYMMETRICAL JOUKOWSKI AIRFOIL 12 PERCENT THICK AND A CYLINDER WITH RADIUS EQUAL TO THE AIRFOIL LEADING EDGE RADIUS.





NATIONAL ADVISORY  
COMMITTEE FOR AERONAUTICS

FIGURE 11.- DISTRIBUTION OF WATER DROPS ON THREE DIFFERENT AIRFOILS WHEN THE DROPS ARE UNDEFLECTED BY FORCES IN THE AIR STREAM.